

Experimental Study on the Vibration Response of a Jackleg Hammer Drill

by

Srividya Kuppa

A thesis

presented to the University of Waterloo

in fulfillment of the

thesis requirement for the degree of

Master of Applied Science

in

Systems Design Engineering

Waterloo, Ontario, Canada, 2025

© Srividya Kuppa 2025

Author's Declaration

I hereby declare that I am the sole author of this thesis. This is a true copy of the thesis, including any required final revisions, as accepted by my examiners.

I understand that my thesis may be made electronically available to the public.

Abstract

This thesis presents an experimental investigation into the **response of mechanical vibration** in jackleg hammer drills during underground rock drilling operations. While previous studies have primarily focused on vibration exposure at the handle or operator interface, this work analyzes vibration transmission through the full structure of the drill to better understand internal component behavior under realistic working conditions. Vibration data were collected using uniaxial accelerometers mounted on four key components—the fronthead, main cylinder, backhead, and handle, with measurements recorded along three spatial axes. Testing was conducted in operational environments, capturing variations across distinct drilling phases, including collaring, sustained drilling, and retraction. The acquired data were processed using time and frequency domain methods, including **Fast Fourier Transform** (FFT) and Root Mean Square (RMS) analysis.

Results revealed significant directional dependence of vibration, with the axial (X-axis) component exhibiting the highest amplitudes during drilling. During collaring, when the drill bit lacks a guiding groove, vibration increased across all axes. A **resonance condition** was observed at approximately 142 Hz in the handle assembly, suggesting localized amplification potentially due to dynamic interaction between structural components. By characterizing **dominant frequencies**, directional behavior, and phase-specific amplification trends, this study provides a system-level understanding of vibration response in jackleg drills. The findings establish a foundation for future research aimed at developing targeted design improvements and vibration mitigation strategies to enhance operator safety and tool performance.

Keywords- Jackleg hammer drill, vibration response, experimental analysis, resonance, hand-arm vibration, underground mining, FFT, directional vibration, drilling phases, operator exposure

Acknowledgements

I am sincerely grateful to my supervisor, **Professor Reem Roufail**, for her unwavering guidance and support throughout this project. Her encouragement and direction were instrumental in shaping this work. I am also deeply grateful to my co-supervisor, **Professor Zia Saadatnia**, for his valuable insights into vibration analysis and his patient mentorship during the technical stages of data acquisition and interpretation.

I would like to sincerely thank **CANUN** and **Mitacs** for funding this research and providing the opportunity to work on a project grounded in real-world impact. Special thanks to **Doug** and **Gates** from CANUN for their support and assistance during field testing; this project would not have been possible without their cooperation.

I would also like to acknowledge the University of Waterloo and the Department of Systems Design Engineering for providing the academic environment and resources necessary to carry out this work.

I am especially thankful for the emotional support and grounding presence of my friends Aishwarya, Sharvari, and Sainath, as well as all my roommates at 185 Pinegrove, who nourished me in every way - from meals to midnight pep talks.

Finally, I owe everything to my family. To my parents, sister, aunt, and granny, thank you for your endless love, encouragement, and belief in me, even when I doubted myself. This journey was never mine alone- it was yours too.

Dedication

To my grandma and uncle, whose absence is felt deeply,

To my grandfather, whose strength and wisdom continue to inspire me, and to my entire family and friends, for the love, faith, and grounding presence that carried me through this journey.

Table of Contents

Author’s Declaration	ii
Abstract.....	iii
Acknowledgements	iv
Dedication.....	v
List of Figures.....	x
List of Tables.....	xii
Chapter 1: Introduction.....	1
1.1 Background of Jackleg Hammer Drills and Industrial Relevance.....	2
1.2 Vibration-related Challenges in Jackleg Drilling	3
1.3 Motivation and Objectives of Research.....	4
Chapter 2 : Literature Review	6
2.1 Occupational Health Risks of Vibration Exposure.....	6
2.2 Regulatory Standards and Thresholds for Vibration Exposure	6
2.3 Measurements and Analysis of Vibration in Rock Drilling.....	8
2.4 Vibration Response in Mechanical Structures.....	9
2.5 Engineering Solutions for Vibration Mitigation.....	10
2.5.1 Grip and Handle Modifications	10
2.5.2 Anti-Vibration Gloves	12
2.5.3 System-Level Redesign and Passive Damping Approaches.....	12
2.6 Gaps in Existing Literature and Need for this Research.....	13
2.7 Research Questions and Hypotheses	14
2.8 Scope and Limitations	16
Chapter 3 : Drill Mechanics and Analytical Framework.....	18

3.1 Mechanical Design and Working Principles	18
3.1.1 Components and Functional Roles	18
3.1.2 Impact and Rotation Mechanisms	22
3.1.3 Parameters Influencing Vibrations	23
3.2 Motivation for Analytical Modelling.....	25
3.3 Four-Lumped Mass Model	26
3.3.1 Schematics with Masses, Springs and Dampers	26
3.3.2 Mass, Stiffness and Damping Matrices	27
3.3.3 Mathematical Formulation of Equations of Motion	30
3.3.4 Generic Force Representations	30
3.3.5 Discussion of Non-Harmonic Periodic Excitation.....	32
3.4 Relations between Model and Drill Components.....	32
3.5 Limitations of the Model	33
Chapter 4 : Experimental Methodology	35
4.1 Purpose of Experimental Work	35
4.2 Experimental Locations and Environment	36
4.3 Equipment and Instrumentation.....	37
4.3.1 Jackleg Hammer Drill.....	37
4.3.2 Test Rig and Mounting Arrangements.....	38
4.3.3 Sensors and Measuring Devices	38
4.3.4 Data Acquisition System	39
4.3.5 Data Acquisition Software.....	40
4.3.6 Safety Equipment	41
4.4 Experimental Protocol and Procedures.....	42

4.4.1 Machine Segmentation and Sensor Placement Strategy	42
4.4.2 Operational Test Configurations.....	43
4.4.3 Measurement Procedures.....	45
4.5 Challenges and Limitations	45
Chapter 5 : Analysis, Results and Discussion	47
5.1 Data Preprocessing and Signal Conditioning	47
5.1.1 Noise Thresholding and Filtering	47
5.1.2 Run Selection and Consistency Verification	48
5.1.3 Configurations for Frequency Analysis.....	49
5.2 Time-Domain Analysis.....	49
5.2.1 Acceleration amplitudes and Component Response.....	50
5.2.2 Observation of Drilling Phases	50
5.2.3 Transient Features and Signal Stability	50
5.2.4 Role of Time-Domain Analysis.....	51
5.3 Frequency-Domain Analysis	51
5.3.1 FFT and Spectral Behavior of Each Component	51
5.3.2 Key Findings and Correlations	53
5.4 Vibration Response and Mapping	54
5.4.1 Directional Propagation Trends.....	54
5.4.2 Resonant Frequency Zones.....	55
5.4.3 Visualization and Mapping.....	55
5.5 Discussion of Results.....	57
5.5.1 Handle Vibration Characteristics.....	57
5.5.2 Backhead Vibration Characteristics	63

5.5.3 Main Cylinder Vibration Characteristics	67
5.5.4 Propagation In X-Axis	72
5.5.5 Propagation In Y-Axis	72
5.5.6 Propagation In Z-Axis	73
5.5.7 Suspected Resonance.....	73
Chapter 6 : Conclusion and Future Work	75
6.1 Summary of Major Findings.....	75
6.1.1 Modeling Insights	75
6.1.2 Experimental Findings.....	75
6.2 Contributions of the Thesis.....	76
6.3 Limitations of the Current Study	77
6.4 Recommendations	77
References	78
Appendix A Test Site and Equipment Images.....	81
Appendix B FFT- Acceleration Magnitude- Frequency Tables	82
Appendix C Stiffness Calculations.....	84

List of Figures

Figure 1.1-1 Jackleg drill operated in the mine. Source- www.canun.com	1
Figure 2.3-1 Test Bench created for testing by Marcotte et al. Source- [10]	8
Figure 2.5-1 The Handle sleeve developed for Vibration Damping, Source- [11]	11
Figure 2.5-2 Vibration Damping Setup by Lindell et al. Source- [16].....	11
Figure 2.5-3 ISO Certified Vibration-Damping Gloves, Source- www.superiorglove.com	12
Figure 3.1-1 Jackleg Drill with Main Components Labeled	18
Figure 3.1-2 The parts of a Jackleg Drill, Source- www.canun.com	19
Figure 3.1-3 Schematic of internal airflow and mechanical structure of the jackleg drill.	19
Figure 3.1-4 Schematic of internal water flow through the jackleg drill.....	20
Figure 3.1-5 Exploded view of the Piston-Rifle bar assembly, along with the valve assembly.....	23
Figure 3.3-1 Low-fidelity 4-mass vibration model of the jackleg drill, showing mass–spring–damper representation with input excitation.	27
Figure 4.2-1 Schematic of sensor placement and data acquisition setup used during jackleg drill testing.	36
Figure 4.3-1 Basic Dimensions of Drill	37
Figure 4.4-1 top view of the jackleg drill instrumented with accelerometers at multiple locations, and X, Y & Z axes defined.....	43
Figure 5.1-1 A Snapshot of the FFT of X-Axis across all Components.....	47
Figure 5.1-2 RMS Acceleration of X-Axis over the period of the test.....	48
Figure 5.4-1 3D surface Heatmap for Vibration across Components and Axis during Collaring.....	55
Figure 5.4-2 3D surface Heatmap for Vibration across Components and Axis during Drilling	56
Figure 5.4-3 3D surface Heatmap for Vibration across Components and Axis during Retraction	56
Figure 5.5-1 Mounted accelerometers on the Handle of the drill, showing orientation relative to the structural axis.	57
Figure 5.5-2 Dominant frequencies and average RMS acceleration in X, Y, Z axes at the handle during collaring phase.	60
Figure 5.5-3 Dominant frequencies and average RMS acceleration in X, Y, Z axes at the handle during drilling phase.....	60
Figure 5.5-4 Dominant frequencies and average RMS acceleration in X, Y, Z axes at the handle during Retraction phase.....	61

Figure 5.5-5 Dominant frequencies and average RMS acceleration in X, Y, and Z axes at the backhead during collaring phase.	65
Figure 5.5-6 Dominant frequencies and average RMS acceleration in X, Y, and Z axes at the backhead during drilling phase.....	65
Figure 5.5-7 Dominant frequencies and average RMS acceleration in X, Y, and Z axes at the backhead during retraction phase.	66
Figure 5.5-8 Dominant frequencies and average RMS acceleration in X, Y, and Z axes at the main cylinder during collaring phase.	69
Figure 5.5-9 Dominant frequencies and average RMS acceleration in X, Y, and Z axes at the main cylinder during drilling phase.....	70
Figure 5.5-10 Dominant frequencies and average RMS acceleration in X, Y, and Z axes at the main cylinder during retraction phase.	70

List of Tables

Table 4.3-2 Specifications of the Uniaxial Accelerometer Used for Field Testing.....	39
Table 4.3-3 Data Acquisition System Specifications	40
Table 4.3-4 DSA Software Settings used in Testing	41
Table 4.4-1 Summary of test runs conducted at full and half throttle settings, showing approximate duration, drill part tested, and axis orientation.	44
Table 5.5-1 Dominant frequencies and RMS acceleration values in X, Y, and Z axes at the handle during Collaring.	61
Table 5.5-2 Dominant frequencies and RMS acceleration values in X, Y, and Z axes at the handle during Drilling.	62
Table 5.5-3 Dominant frequencies and RMS acceleration values in X, Y, and Z axes at the handle during Retraction.	62
Table 5.5-6 Dominant frequencies and RMS acceleration values in X, Y, and Z axes at the backhead during retraction phase.	67
Table 5.5-7 RMS acceleration values at dominant frequencies in X, Y, and Z axes at the main cylinder during collaring phase.	71
Table 5.5-8 RMS acceleration values at dominant frequencies in X, Y, and Z axes at the main cylinder during the drilling phase.	71
Table 5.5-9 RMS acceleration values at dominant frequencies in X, Y, and Z axes at the main cylinder during the retraction phase.	71

Chapter 1

Introduction

Jackleg Hammer drills are widely utilized percussion tools in the mining industry for rock drilling to blast holes or install ground support in underground mines where larger machines cannot operate. They are considered essential due to their portability, adaptability and sustainability under restricted operating conditions. These drills are designed to apply rotational and impact forces to penetrate the rock surfaces efficiently with a steel drill bit, which is struck repeatedly by a piston in a pneumatic cylinder. The retractable airleg attached to the drill helps stabilize and position the drill to enhance precision and accuracy during drilling operations. This drill is extremely convenient due to its placement of critical controls- essential for both the airleg and the drill, at the handle to ensure that operators have a firm grip on the drill during the operations, as shown in Figure 1.1-1. [1]



Figure 1.1-1 Jackleg drill operated in the mine. Source- www.canun.com

During the initial stage, known as *collaring*, the operator must exert significant physical effort to start the hole. This phase lasts 5-10 seconds and requires a tight grip on the handle to stabilize the

drill and adjust the air leg. The peak effort is observed here, where miners may exert forces ranging between 50 to 100 N, depending on the rock hardness and operator strength [1].

Once the hole is established, the *drilling* phase proceeds with reduced manual intervention. The operator typically releases the tight grip on the handle and allows the airleg to support the drill, although they remain nearby to monitor performance. The *retraction* phase follows once the desired depth is achieved, typically around 76 cm (during testing) for a 60-80 second drilling cycle. Here again, the operator actively controls the handle to reposition the airleg, a process that takes 5-15 seconds.

The jackleg drill's impact frequency reaches up to 2250 blows per minute (bpm), corresponding to approximately 37.5 Hz at full throttle. In practice, vibration measurements from this study revealed dominant frequency peaks around 35–36 Hz at full throttle and 21–23 Hz at partial throttle.

Prolonged exposure to such intense vibrations is known to cause serious issues, including peripheral vascular disorders, along with neurological and musculoskeletal conditions, collectively classified as Hand-Arm Vibration Syndrome (HAVS) [1], [2]. These conditions significantly impact operators' health, productivity and overall quality of life. The prevalence of such impacts mandates the establishment of rigorous occupational health standards, such as ISO 5349. These guidelines set clear permissible exposure limits and emphasize the critical need for effective vibration mitigation in pneumatic drilling tools.

1.1 Background of Jackleg Hammer Drills and Industrial Relevance

Historically, jackleg drills emerged in the early to mid-20th century, providing a portable solution for drilling in environments where larger drills were impractical. These drills operate on compressed air, which powers an internal piston that strikes a drill steel bit, generating a percussive impact that fractures the rock. At the same time, a rotational mechanism advances the bit, allowing the drill to bore effectively into the substrate. Their ability to function without electricity makes them particularly suitable for remote or underdeveloped mining operations where power infrastructure is limited.

One of the primary advantages of the drill is its versatility. They are preferred for horizontal or near-horizontal tunnelling through the rock because of their mobility and adjustability. The airleg enables operators to maintain consistent contact and force on the drill, even when working at

awkward angles or heights. This feature also helps stabilize the drill and reduces the physical strain on the operator, though it still generates high levels of vibration that can pose ergonomic risks.

Despite the rise of more automated and large-scale drilling rigs, jackleg drills continue to play a crucial role in the mining industry. They are especially valuable in narrow vein mining, development headings, and exploratory drilling, where space is limited and flexibility is key. According to the Mine Safety and Health Administration (MSHA), jackleg drills are still widely used in the North American mining sector, particularly in older or smaller mines where more expensive equipment may not be practical. Additionally, many mining training programs consider jackleg drill operation a fundamental skill for underground miners [3].

1.2 Vibration-related Challenges in Jackleg Drilling

Even though the drill is an indispensable tool in underground mining, a significant operational challenge arises from the intense mechanical vibrations transmitted to the user's hands and arms during use. These vibrations stem from the mechanisms in the drill, which are essential for enhancing productivity. The resulting vibrations pose considerable risks to both the health of the operators and the longevity of the tools themselves.

One of the important concerns for operators is exposure to Hand-Arm vibration, commonly known as HAV. Prolonged or frequent exposure to HAV can lead to Hand-Arm Vibration Syndrome (HAVS), a condition that impacts the circulatory and neurological systems and includes musculoskeletal disorders. Numbness, tingling, reduced grip strength, and, in more advanced cases, episodes of finger blanching, often referred to as "white finger," due to compromised blood flow, are some of the symptoms of HAVS. If left untreated, HAVS can lead to permanent disability, severely impacting a worker's ability to perform even basic manual tasks. [4]

Other than the health risks to the workers, the vibration forces generated by the drills significantly contribute to the tool wear and fatigue. Continuous exposure to the high-frequency impacts creates fatigue cracks in critical components like the piston, chuck driver, bushing, etc. and propagates throughout the drill, ultimately leading to reduced tool lifespan and an increase in maintenance demands. This increases the operational costs and also increases safety hazards, as any component could fail during drilling operations.

Regulatory bodies around the world have acknowledged these risks and have established standards aimed at limiting vibration exposure. Guidelines like ISO 5349-1 describe methods for measuring hand-arm vibration and propose exposure limits aiming to minimize the likelihood of developing HAVS. In North America, organizations such as OSHA- Occupational Safety and Health Administration and the Mine Safety and Health Administration (MSHA) have formulated additional regulations and recommendations for managing vibration exposure in industries that use hand-held tools. [5]

Numerous engineering and administrative controls have been devised to counter these challenges. Some of the modern jackleg drills feature vibration-damping handles, improved tool balance, but literature shows that these additions are not very effective and prove to be a hindrance to the operator and affect their efficiency. Equally important are administrative measures such as limiting daily exposure duration, rotating tasks among workers to distribute the workload, and implementing health surveillance programs to detect early signs of HAVS [6].

1.3 Motivation and Objectives of Research

Despite technological advancements, vibration exposure continues to present a persistent challenge in mining environments that rely on handheld pneumatic tools such as jackleg drills. These tools generate significant mechanical vibration during operation, particularly at the beginning and end of the drilling cycle, which is physically demanding for the operator. Over time, this exposure can contribute to musculoskeletal fatigue, compromised grip strength, and long-term health effects classified under Hand-Arm Vibration Syndrome (HAVS).

Field attempts to mitigate vibration through engineering interventions, such as damping sleeves or redesigned handles, have often failed under real operational conditions. In one notable case, CANUN partnered with a third-party firm to develop a vibration-damping handle; operators expressed dissatisfaction with the added stiffness and loss of handle flexibility. Similarly, with the vibration-damping gloves, the project was discontinued after materials used in the prototype began to peel off during underground operation and has seen limited success due to poor ergonomics and durability.

While regulatory standards such as ISO 5349 define acceptable daily vibration exposure limits, the effectiveness of real-world solutions remains questionable in harsh and variable underground conditions. This underscores the need for a deeper, system-level understanding of how vibration

propagates through the tool, both in frequency and direction, before practical solutions can be effectively designed.

The objective of this research is to bridge that gap. Instead of focusing directly on mitigation, this study aims to characterize the nature of vibration exposure through field experiments and detailed analysis of vibration behavior at different parts of the jackleg drill.

Research Objectives

- To quantify the dominant frequencies and vibration amplitudes experienced at key structural points on the jackleg drill during operation.
- To analyze the directional behavior of vibration (X, Y, Z axes) across components such as the fronthead, main cylinder, backhead, and handle.
- To identify potential system-level amplification effects, including frequency-specific behaviors that may relate to dynamic transmission.
- To evaluate how vibration changes across operational phases, particularly collaring, sustained drilling, and retraction.
- To establish a foundational dataset and understanding that can inform future efforts aimed at reducing operator exposure.

Chapter 2: Literature Review

2.1 Occupational Health Risks of Vibration Exposure

Prolonged exposure to mechanical vibration is a significant occupational hazard, particularly in industries that rely heavily on handheld percussive tools such as rock drills. In the mining sector, workers operating jackleg hammer drills are among the most affected, as they are routinely exposed to high-magnitude, impulsive forces transmitted directly through the tool into the hands, wrists, and arms.

Extended exposure to such vibration has been linked to the development of Hand-Arm Vibration Syndrome (HAVS)- a progressive, often irreversible condition characterized by vascular, neurological, and musculoskeletal impairments. Symptoms range from tingling and numbness to reduced grip strength, particularly Vibration-induced White Finger (VWF). In severe cases, it might lead to permanent loss of manual function, effectively limiting a person's capacity to handle tools, write, button clothing or carry objects [4] .

According to ISO 5349-1 and ISO 5349-2, workers exposed to vibration levels above 2.5 m/s^2 (action value) face significant long-term risks, with levels exceeding 5 m/s^2 (exposure limit) associated with a high risk of HAVS onset. These values have been adopted in regulatory frameworks worldwide, forming the basis for exposure monitoring and safety guidelines. Anecdotal accounts from veterans in the industry, particularly those who worked in mines before widespread regulations were implemented, highlight the consequences of long-term exposure without protective practices. In some cases, workers were forced to retire early due to disabling symptoms. [7], [8]

HAVS is recognized as a permanent occupational illness, for which there is no known cure, only preventive measures. Beyond the health issues, affected workers may experience reduced productivity and income, and employers have to face increased operational costs due to compensation claims, reduced crew efficiency, and difficulty in maintaining long-term workforce capacity. [2], [4]

2.2 Regulatory Standards and Thresholds for Vibration Exposure

International Standards and National safety agencies have established exposure thresholds, measurement methodologies, and control guidelines to mitigate the health risks associated with Hand-

Arm Vibration. These frameworks are crucial in defining what constitutes excessive vibration and how it should be measured and managed in industrial environments.

Among the most widely adopted standards are those issued by the International Organization for Standardization (ISO). ISO 5349-1 and ISO 5349-2 outline both the technical procedures for measuring vibration and the recommended daily exposure thresholds. The standardized limits are based on an 8-hour equivalent daily exposure (A(8)):

- 2.5 m/s² - Action Value: employers must implement monitoring and take steps to reduce exposure.
- 5.0 m/s² – Exposure Limit Value: beyond this, the chance of developing HAVS is significantly increased, and continued exposure is considered unsafe [7], [8].

In the context of mining operations, especially jackleg drilling, measured vibration levels often exceed these thresholds, depending on tool condition, rock hardness, operator technique, and drilling phase. Exposure at or above these levels is not uncommon during full-shift operations and can contribute to long-term injury, early retirement, or loss of hand functionality.

In North America, agencies such as the Occupational Safety and Health Administration (OSHA) and the Mine Safety and Health Administration (MSHA) provide educational guidance and training resources that encourage safe handling practices and awareness. MSHA's modules for jackleg drills encourage frequent tool checks and ergonomic posture to reduce risk, although they do not impose legally binding numeric limits.

These standards define precise methods for evaluating hand-transmitted vibration, including triaxial acceleration measurement, frequency weighting, and sensor placement guidelines. They also outline the procedure for analysis, including the use of frequency weighting filters, RMS-based averaging. In this study, three uniaxial accelerometers were mounted orthogonally on different components of the drill to capture vibration in the X, Y, and Z axes. This setup approximates an ISO-aligned measurement by enabling directional analysis while compensating for the lack of a single triaxial sensor. The mounting locations and methodology were chosen to reflect realistic operator exposure.

2.3 Measurements and Analysis of Vibration in Rock Drilling

Accurate vibration measurement is essential for evaluating the safety and ergonomic performance of jackleg hammer drills. Most studies to date have focused on vibration levels at the handle, where contact with the operator occurs, using variations of tool-attached or hand-attached accelerometer setups. These studies serve as foundations for understanding operator exposure and validating compliance with regulatory limits, though they primarily focus on single-point measurement.

Keith and Brammer [9] investigated vibration exposure during jackleg drilling by measuring accelerations at the handle using tool-mounted sensors. Their results showed that under realistic working conditions, exposure levels often exceeded ISO thresholds, especially during full load drilling phases, posing a high risk for HAVS. They concluded that reliable field measurement was essential for establishing safe work limits and highlighted the role of tool condition and operator technique in influencing vibration magnitudes.

Clemm et al. [6] compared hand-attached and tool-attached accelerometer mounting methods on pneumatic rock drills. They found that tool-attached sensors often underestimated the true vibration experienced by the operator, especially under impulsive percussive forces. Their findings led to important recommendations on sensor placement, emphasizing the need for representative measurements aligned with hand-transmitted vibration standards.

Marcotte et al. [10] developed a controlled test bench for jackleg hammer drill models and operating conditions, as shown in Figure 2.3-1. Their setup allowed for repeatable testing in a lab environment, eliminating operator variability. The study confirmed that factors such as air pressure, drill steel condition, and lubrication significantly influenced vibration levels. However, they also acknowledge that bench testing alone could not fully replicate in-situ rock drilling dynamics.



Figure 2.3-1 Test Bench created for testing by Marcotte et al. Source- [10]

The MIRARCO study [11] extended this work to the field, capturing handle vibration during real drilling tasks performed in underground environments. Their analysis showed that tool orientation, rock hardness, and operator handling style all affected both the amplitude and direction of vibration. The study also highlighted significant variability in measured exposure levels, even within the same tool model, emphasizing the importance of field-based data to supplement laboratory measurements.

In a different context, Fang et al. [12] investigated how vibration data can be utilized to detect rock layer transitions and changes in lithology during rotary-percussive drilling. Although their work was not focused on hand-arm vibration, it demonstrated the diagnostic potential of vibration signals and their sensitivity to structural and material variations during drilling.

These studies demonstrate the value of vibration measurement in assessing both health risks and operational performance. They also explain how tool condition, operator technique, and environmental factors can influence measurement outcomes. Most existing research, however, has focused primarily on vibration at the handle, establishing a baseline for health-focused assessments and regulatory compliance in jackleg drill use.

2.4 Vibration Response in Mechanical Structures

Research on vibration exposure in handheld percussive tools, including jackleg drills, typically emphasizes measuring vibrations at the tool-operator interface. However, effective vibration control requires a comprehensive understanding of how vibrations propagate internally through structural components, affecting vibration characteristics experienced at the user interface.

Vibration response involves the transfer of dynamic mechanical energy through interconnected structural elements, influenced by factors such as geometry, material properties, and the interface between components [13]. During propagation, vibrations can undergo significant changes, including amplification, attenuation, or resonance, affecting operator exposure and ergonomic design.

While explicit studies examining internal vibration response in Jackleg drills remain limited, relevant methodologies from studies in other mechanical systems can provide valuable insights. For instance, Reksoprodjo and Nirbito [14] studied vibration propagation characteristics on a passenger car's monocoque body structure using multi-point vibration measurements and frequency-domain analysis methods. Their research demonstrated that vibration propagated from the engine mounting points through various structural interfaces, experiencing both amplification and attenuation

depending on the structural configurations and the connection between components. Significant frequency-dependent behaviors were observed, illustrating how structural designs impact vibration transmission paths and severity at user contact points.

The principles highlighted by Reksoprodjo and Nirbito align closely with the fundamental concepts in mechanical vibration literature, particularly regarding structural resonances and frequency-dependent propagation effects [13], [15]. Structural resonance occurs when excitation frequencies match the component's natural frequency, significantly amplifying vibration amplitudes, thereby increasing potential harm to operators. Identifying these resonance conditions generally requires systematic, multi-point measurement and frequency-domain analysis throughout the structure.

2.5 Engineering Solutions for Vibration Mitigation

Several engineering strategies have been proposed over the years to reduce the risk of hand-arm vibration exposure in hand-held percussive tools, including anti-vibration gloves, handle modification, and system-level damping interventions. While these approaches offer some level of vibration reduction under controlled conditions, their real-world effectiveness is often limited by ergonomic factors, user rejection, or implementation challenges in difficult working environments.

2.5.1 Grip and Handle Modifications

A joint private study by MIRARCO and CANUN International evaluated a series of prototype damping grips, as shown in Figure 2.5-1, on a jackleg drill using four different durometer ratings (27, 40, 50, 60) and compared them to a steel handle. The grip with a 50-durometer rating demonstrated the best performance, with up to 41% vibration reduction in the X-axis (axis of drilling) during field drilling on Norite rock. Despite this improvement, overall peak acceleration levels remained high (48–86 m/s²), and no formal usability evaluation was conducted. According to anecdotal insights from technicians, the prototype handles were ultimately rejected in practice due to poor ergonomics during extended use[11].



Figure 2.5-1 The Handle sleeve developed for Vibration Damping, Source- [11]

Kremer et al. [2] reinforced this disconnect between design and field reality in a pilot study assessing ergonomic hazards of jackleg drills. They reported that users continued to experience discomfort, regardless of whether vibration-reduction features were incorporated. Their findings showed that operator technique, tool orientation, and the constrained underground environment significantly impacted perceived vibration, often overriding any static design improvements.

Building on this, Lindell et al. [16] presented a system-level redesign of a pneumatic rock drill for rock stabilization. Their innovation combined a suspended handle, spring-damper system, and a non-linear auto-tuning vibration absorber (ATVA) integrated into the hoist. This setup, shown in Figure 2.5-2, reduced vibration from 34.6-40.8 m/s^2 to 11.6 m/s^2 at the handle, and from 25.4-40.9 m/s^2 to 5.4 m/s^2 at the hoist lever. Although promising, the redesigned system increased tool weight by over 5 kg, which may hinder adaptation in truly handheld tools.



Figure 2.5-2 Vibration Damping Setup by Lindell et al. Source- [16]

2.5.2 Anti-Vibration Gloves

Anti-vibration gloves (AVGs) are commonly marketed as a simple solution to reduce exposure to harmful vibration. However, Maeda et al. [17] found that even ISO 10819-certified gloves, shown in Figure 2.5-3, failed to reliably attenuate vibration at the wrist under real operating conditions. Using a novel on-body measurement technique, they observed that glove transmissibility varied depending on grip force and excitation frequency, both of which are inconsistent in field use.



Figure 2.5-3 ISO Certified Vibration-Damping Gloves, Source- www.superiorglove.com

In a separate study, Tirabasso et al. [18] tested three gloves, both in lab and field settings. Two of the gloves amplified vibration in field use, despite meeting ISO criteria in laboratory tests. The researchers concluded that real-world hand-transmitted vibration differs significantly from standardization conditions, making glove certification a poor proxy for actual protection. These results raise concerns about relying on AVGs as a primary line of defense, particularly in percussive tasks like jackleg drilling.

2.5.3 System-Level Redesign and Passive Damping Approaches

Some researchers have pursued structural and model-informed vibration reduction strategies to move beyond surface-level interventions. Le et al. [19] applied a top-down design method to create a modular Tuned Mass Damper (TMD) for handheld hammer drills. Their impedance-targeted approach achieved a 47% reduction in vibration at key frequencies, validated through analytical models and test bench measurements. Though the drill type was electric rather than pneumatic, the design principles, particularly isolating system resonance through passive damping, apply to jackleg drills.

Savilov et al. [20] reviewed a wide range of vibration suppression techniques in high-performance drilling, emphasizing the value of viscoelastic inserts, spring-damper couplings, and passive absorbers. However, they noted that size, weight, and mechanical durability remain critical challenges when adapting these components for handheld tools used in heavy-duty environments.

2.6 Gaps in Existing Literature and Need for this Research

The occurrence of hand-arm vibration exposure among operators of the jackleg drill, despite decades of engineering efforts, reveals a critical disconnect between existing mitigation strategies and field realities. While several mechanical and ergonomic interventions have been explored, they often fail due to technical limitations in real-world conditions.

As seen in the MIRARCO-CANUN handle redesign study, even the best-performing grip material reduced vibration by only 41% under limited conditions and failed to bring exposure within ISO-defined safe limits. More importantly, the damping handle was ultimately rejected by operators due to poor ergonomic comfort and its disruptive effect on operations during extended use. Similarly, the pilot study by Kremer et al. [2] confirmed that vibration-related discomfort persisted in underground mining settings regardless of minor design improvements, largely due to the dynamic and constrained nature of the working environment, which shadows fixed physical countermeasures.

Anti-vibration gloves (AVGs), while accessible and commonly used, also fall short. Experimental work by Maeda et al. [17] and Tirabasso et al. [18] showed that gloves certified under ISO 10819 frequently failed to protect operators under realistic task conditions and, in some cases, amplified vibration levels. These results clearly demonstrate that laboratory compliance is not a sufficient predictor of field effectiveness, especially in high-impact, multi-directional vibration environments such as jackleg drilling.

Even more sophisticated redesigns, such as the suspended handle and nonlinear vibration absorber system proposed by Lindell et al. [16], have shown promising vibration reduction, achieving up to 70% decrease in RMS levels, but increase the tool weight and complexity. These systems may work in semi-mechanized setups but remain impractical for manually operated tools where mobility and control are critical.

Other studies, like the top-down TMD-based redesign by Le et al. [19], and the vibration suppression review by Savilov et al. [20], demonstrate the potential of system-level design and

modular passive damping. However, these approaches are rarely applied to pneumatic drills and are often validated only in idealized or lab-based conditions. Crucially, most of them only focus on vibration at the handle without assessing how vibration is generated and transmitted internally across different components.

There remains a clear gap in understanding how vibration propagates through the internal structure of the jackleg drill, how impacts from the piston travel through the fronthead, main cylinder, backhead, and ultimately to the handle. The lack of component-level or system-level vibration analysis prevents designers from identifying where and why vibration is amplified, and how tool design might be optimized to address these root causes.

This research addresses the gap by:

- Conducting multi-axis, multi-point vibration measurements under realistic operational conditions,
- Identifying dominant frequencies and possible resonance behaviors in structural components,
- And laying the foundation for future model-based design improvements through initial system-level analysis.

Rather than relying solely on end-point vibration reduction (e.g. gloves or damping handles), this thesis shifts the focus toward understanding how vibration is distributed and amplified within the tool, a perspective that is currently missing in both academic literature and industrial practice.

2.7 Research Questions and Hypotheses

As outlined in the previous sections, most of the existing studies on jackleg drills focus on measuring vibration only at the operator's handle. While such data is important for evaluating health risks, it does not offer insight into how the vibration is generated, how it travels through the drill's internal structure, or why certain components may amplify it. Without this level of understanding, attempts at vibration mitigation remain limited to surface-level interventions, which are either ergonomically unsuitable or technically insufficient in the field.

To address this gap, this study investigates the vibration characteristics of a jackleg hammer drill using multi-axis, multi-point acceleration measurements under realistic operating conditions. By

capturing data from different structural components, specifically the fronthead, main cylinder, backhead, and handle, the research aims to understand how vibration propagates across the system and reaches the operator.

The study is guided by the following research questions:

1. What are the dominant vibration frequencies and amplitudes experienced during jackleg drill operation, and how do they vary across different components and directions (X, Y, Z)?
2. Are there specific components or structural paths within the drill where vibration is amplified, suggesting internal transmission effects or potential resonance conditions?
3. How does the vibration evolve or transform as it travels from the source of impact (Piston in Main cylinder) toward the operator's hand at the handle?

These questions focus on mapping the dynamic behavior of the drill through experimental evidence.

Based on these, the following hypotheses are proposed

- H1: Certain components of the jackleg drill, such as the handle or backhead, may experience higher vibration amplitudes compared to others, potentially due to how vibration is transmitted internally.
- H2: Distinct frequency components might be consistently observed across multiple parts of the drill, indicating possible transmission patterns or dynamic behaviors worth further investigation.
- H3: The way vibration propagates from the impact source through the drill body is likely influenced by structural factors and may vary directionally across different axes.

These hypotheses are intentionally exploratory and do not assume deterministic outcomes. Rather, they reflect areas where field observations and initial analysis suggest deeper investigation is warranted.

2.8 Scope and Limitations

This study focuses on the experimental investigation of vibration response in a jackleg hammer drill used in underground operations. The primary objective is to measure and analyze how vibration travels through different structural components of the drill- specifically the fronthead, main cylinder, backhead and handle- during actual drilling conditions. The analysis includes identification of dominant frequencies, amplitudes, and directional trends across multiple axes to better understand how vibration is transmitted from the internal impact source to the operator interface.

The scope of the study is limited to:

- A single drill type and manufacturer (CANUN International- Jackleg Drill 260B),
- A field-based testing environment using four uniaxial accelerometers mounted at multiple locations,
- And a data-driven analysis approach without any modification to the tool or operational setup.

This work does not involve:

- Detailed modal analysis or system identification using frequency response functions,
- Finite element modeling or dynamic structural simulation of the drill,
- Redesign, manufacturing, or validation of damping components,
- Or long-term ergonomic trials involving human participants.

Several practical limitations are acknowledged:

- Field conditions introduced variability in data due to changing rock properties, environmental noise, and operator technique.
- Sensor placement was occasionally constrained by tool geometry and mounting stability.
- The study represents a snapshot of short-term vibration behavior and does not quantify fatigue, usability, or cumulative exposure risk.

Despite these constraints, the study provides insight into internal vibration behavior- offering a foundation for future tool design and component-level mitigation strategies.

The remainder of this thesis is organized as follows:

Chapter 3- Drill Mechanics and Analytical Framework - This chapter introduces the internal mechanical structure and operating principles of the drill, along with the theoretical background relevant to vibration transmission.

Chapter 4- Experimental Methodology - This chapter describes the field-testing setup, sensor mounting strategy, data acquisition process, and signal preprocessing methods.

Chapter 5- Analysis, Results, and Discussion - This chapter presents the processed vibration data, including dominant frequencies, RMS values, and directional trends observed across components and phases. The discussion interprets these findings in the context of structural vibration behavior, potential amplification effects, and future design strategies.

Chapter 6- Conclusions and Future Work – The final chapter summarizes the major findings, discusses the limitations of the study, and outlines potential directions for future research.

Chapter 3: Drill Mechanics and Analytical Framework

3.1 Mechanical Design and Working Principles

3.1.1 Components and Functional Roles

The machine used in this study is the CANUN 260B Jackleg Drill, a pneumatically powered handheld drilling tool commonly used in narrow-vein and underground operations. The CANUN 260B delivers high penetration rates with an impact frequency of 2250 blows per minute, a cylinder diameter of 79.4 mm, and a piston stroke of 73.25 mm. These characteristics contribute to its high torque and strong percussive output, making it effective in hard rock environments.

This drill operates through the coordinated function of three main systems:

- Pneumatic actuation system
- Hydraulic support system
- Mechanical Housing and Support System

Each of these systems plays an important role in facilitating efficient drilling, while the internal structure of the tool governs the dynamics of force transmission and vibration. For the ease of understanding of the drill, there are four primary components involved in vibration analysis. The Fronthead, Main cylinder, Backhead, and the Handle are described below in Figure 3.1-1, along with an overview of their respective functions within these systems.

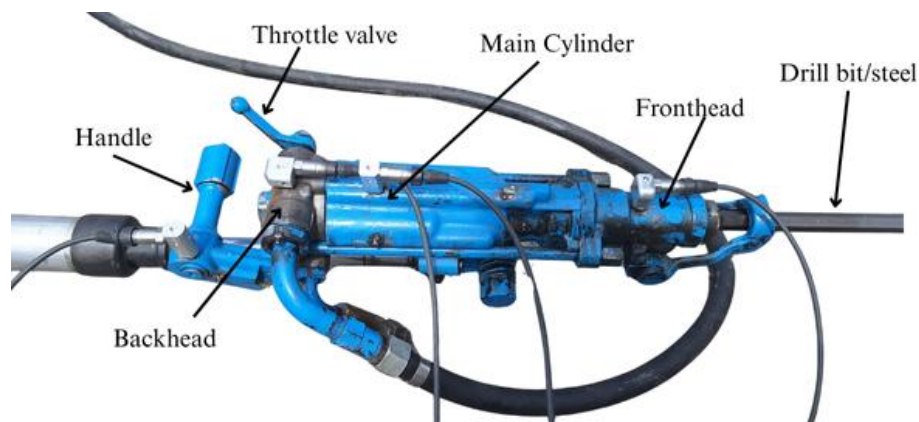


Figure 3.1-1 Jackleg Drill with Main Components Labeled

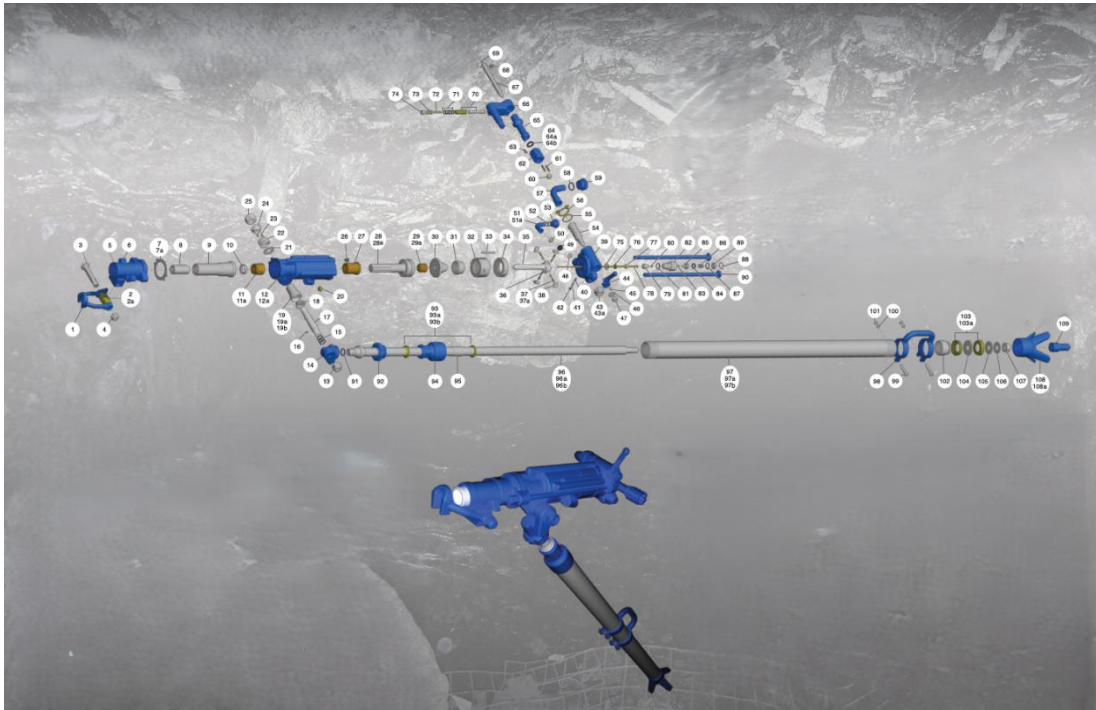


Figure 3.1-2 The parts of a Jackleg Drill, Source- www.canun.com

3.1.1.1 Pneumatic Actuation System

The pressurized air circuit serves as the primary power source for the drill. Compressed air is supplied from an external compressor through a pipeline connected to the backhead, where it flows through internal channels and is regulated by the throttle valve operated by the user. The schematic of the system is shown in Figure 3.1-3.

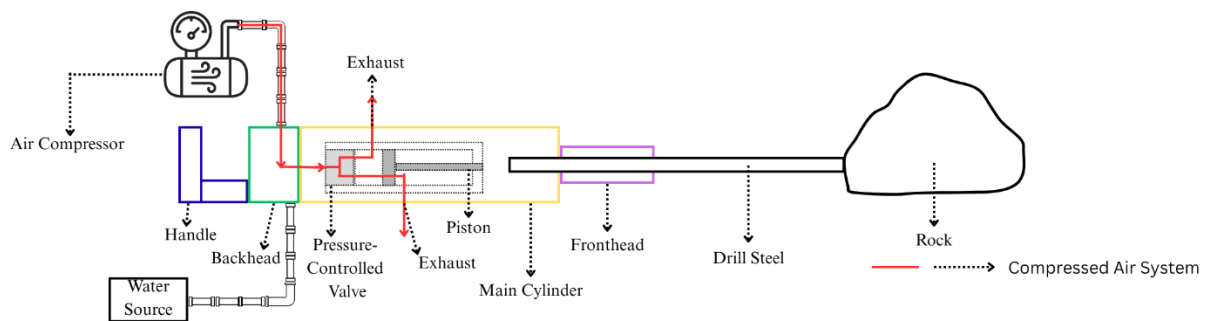


Figure 3.1-3 Schematic of internal airflow and mechanical structure of the jackleg drill.

Once within the valve, the air is alternately directed to each side (behind and in front) of the piston, initiating its reciprocating motion. During the forward stroke, the piston has a significant impact on the drill steel, which is held in place by the Fronthead. This force on the drill steel ensures effective penetration of the rock.

On the return stroke, compressed air is routed to the front of the piston, and the mechanism involving the piston, rifle bar and the ratchet ring ensures the piston is rotated by 10.29° , preparing it for the next indexed strike. This dual functionality facilitates both powerful impacts and ensures the drill remains ready for later operations with high efficiency. The cycle is completed as the compressed air is exhausted through designated outlets.

3.1.1.2 Hydraulic Support System

The hydraulic system plays a vital role in ensuring thermal and operational stability during drilling. Cool water is introduced through the water inlet pipe attached to the Backhead, then it flows through a specified channel towards the drilling steel. This continuous stream serves multiple purposes, including cooling the drill bit/drill steel, removing the rock debris, and mitigating the risks of overheating and sudden rock fractures. This circuit, as shown in Figure 3.1-4, contributes significantly to both safety and operational efficiency.

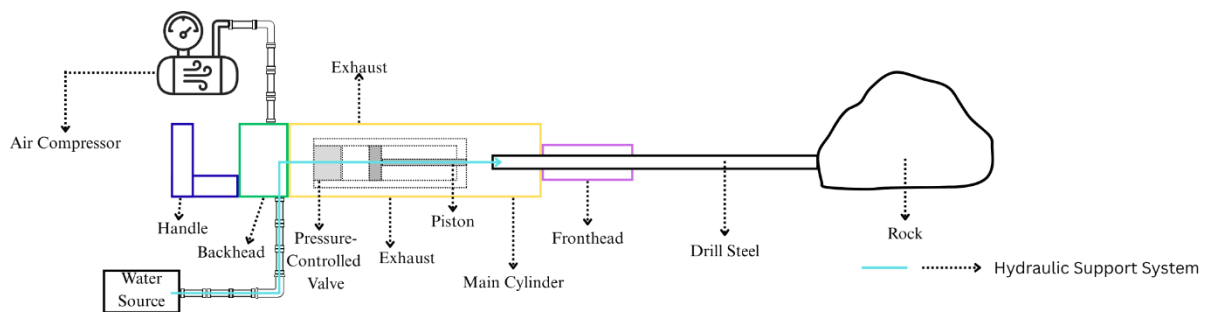


Figure 3.1-4 Schematic of internal water flow through the jackleg drill.

3.1.1.3 Mechanical Housing and Support System

The mechanical architecture of the drill is meticulously designed to support and channel the forces generated by the piston, to effectively transfer both impact and rotational motion to the drill steel. Within this framework, several critical components work in coordination to optimize drilling performance and efficiency. For this study, the system can be divided into four main components:

1. Fronthead- The foremost component of the system, the Fronthead as a mass provides stability. It houses an alignment mechanism for the drill steel to rotate and reciprocate the motion of the piston. It is designed to transmit axial impacts generated during the reciprocating motion of the piston in the cylinder and to transmit the rotational torque. Furthermore, it is also designed to redirect all the reactive forces into the body of the drill.
2. Main Cylinder- houses most of the components of the drill, especially the essential ones. It accommodates the valve assembly, rifle bar, and piston assembly. Its most important function is to aid the pressure-controlled valve that regulates the airflow and directs it to each side of the piston, thereby controlling its movement and impact generation. The rifle bar is another designed component whose function is to induce a rotational movement to the piston during the return stroke. It ensures that the drill bit advances in a controlled manner. The ratchet ring plays a pivotal role in this mechanism, as it locks the rifle bar's position- and subsequently the piston's angle during the forward stroke, permitting a stepwise rotation that is crucial for effective indexing and precision in drilling.
3. Backhead- is attached to the rear end of the cylinder and connects essential components such as air and water inlet ports to the machine, and comprises complex internal pathways designed to direct flow efficiently to the cylinder for the piston as well as the airleg. The manually operated throttle valve is strategically positioned in this region, which helps regulate the volume of air that is permitted into the valve assembly and directly influences the frequency and power of the impacts delivered by the piston. The backhead also channels compressed air to actuate the airleg, thereby enabling precise control over the feed mechanism during the drilling operation.
4. Handle- provides physical control over the drill for the operator. A directional control valve is designed into the handle, allowing the operator to seamlessly switch the air supply to the airleg to extend or contract the piston, depending on the drilling position. This design allows the operator to manually apply forward force, particularly during alignment procedures or at the Collaring stage, i.e. initiation of the drilling process.
5. Airleg- Although the airleg is not integrated into the system considered for the study of vibration response, it plays a crucial role in providing forward thrust during drilling operations. Actuated pneumatically, the airleg extends the drill into the rock, reacting

accurately to the pressured air that is routed from the backhead through the main cylinder. Its design is essential for effective feed control, influencing both the depth and efficiency of the drilling process.

Collectively, these components interact dynamically to create a robust mechanical system capable of delivering high-impact, precise rotational motion, optimizing the overall drilling performance.

3.1.2 Impact and Rotation Mechanisms

The jackleg drill functions through two coordinated mechanisms- Impact and Rotation, both driven by compressed air. These mechanisms work in tandem to fracture the rock by repeated impact loading and grinding due to the rotation of the drill bit at the specific location on the targeted rock and precise drill bit reorientation.

3.1.2.1 Impact Mechanism-

In this mechanism, compressed air enters the main cylinder through a pressure-controlled valve assembly, causing the piston to move in a reciprocating motion. The forward stroke of the piston transmits a concentrated axial impact to the drill steel, while the return stroke readies it for the next cycle. This process occurs at approximately 2250 blows per minute (BPM), or 37.5Hz, imparting significant energy to both the drill and the rock being drilled.

3.1.2.2 Rotation Mechanism-

Alongside impact, the drill steel experiences indexed rotation through an internal rifle bar and ratchet ring assembly. As the piston retracts, it rotates along the rifle bar spline, which the ratchet ring secures during the forward stroke. This stepwise rotation ensures that the drill bit changes orientation after each impact, promoting even pulverization of the rock surface and reducing the risk of jamming. This passive rotation is mechanically synchronized with the piston's movement to enhance the overall drilling efficiency.

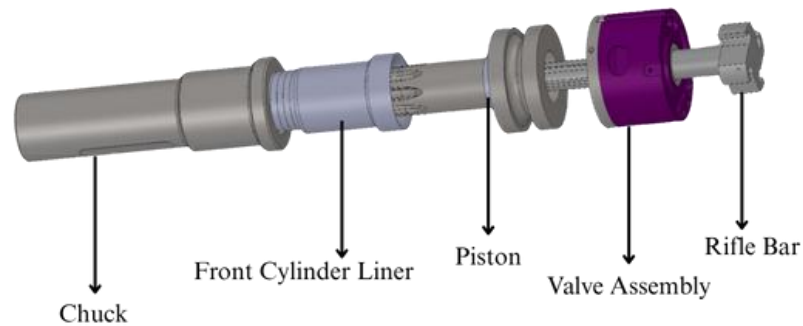


Figure 3.1-5 Exploded view of the Piston-Rifle bar assembly, along with the valve assembly.

3.1.3 Parameters Influencing Vibrations

The intrinsic design and operational mechanisms of the drill introduce a variety of factors that significantly generate mechanical vibrations in the system. These factors arise from the internal characteristics of the system as well as the external conditions under which it operates. A comprehensive understanding of these contributors is essential for developing an analytical model and the subsequent understanding of dynamic responses.

3.1.3.1 Input Force Characteristics

The primary source of vibration in the jackleg drill is the piston, which provides periodic axial impacts to the drill steel. The frequency and amplitude of these impacts are influenced by several parameters, including air pressure, valve timing, and the mass of the piston. Operating at approximately 2250 blows per minute (37.5 Hz), the piston introduces consistent and repetitive excitation into the system, thereby playing a crucial role in the dynamic behavior of the drill.

3.1.3.2 Mechanical Interfaces and Contact Conditions

The drill consists of a series of interconnected external components, such as the Fronthead, main cylinder, backhead, and handle, which are assembled through various methods, including threaded connections, shrink-fit joints, and gaskets. The Fronthead-Main Cylinder are connected by studs and

bolts, same as the Main Cylinder-Backhead joint. The Handle is connected to the Backhead by a shrink-fit joint and a bolt. This type of connection helps the handle to rotate about the horizontal axis and still stay connected to the Backhead without sliding out. The effectiveness of these interfaces, characterized by contact stiffness and the presence of potential micro-gaps or looseness, can introduce compliance and non-linearity. These factors ultimately affect the transmission and amplification of vibrations throughout the drill structure.

3.1.3.3 Mass and Stiffness Distribution

The disparities in mass and stiffness throughout the drill have a profound impact on energy propagation. The main cylinder, situated centrally, exhibits higher rigidity and will react differently compared to the handle, which is more flexible due to the type of connection to the backhead and positioned at the opposite end from the primary impact source. Such structural variances influence the local vibrational modes and increase the likelihood of amplification at specific frequencies.

3.1.3.4 Component Geometry and Spatial Arrangement

The configuration of the drill approximates a cantilever structure, where the impact source is located closer to the constrained end (with the drill bit supported by the rock and the airleg resting against the ground) and the handle is positioned at the free end. This spatial distribution suggests that components such as the handle, which are most distant from the source of impact, may experience higher displacement amplitudes under certain operational conditions [13].

3.1.3.5 External Boundary Conditions

Several external factors, like the grip of the operator on the handle [2], [11], the stiffness of the supporting handle and the extension of the airleg, significantly influence the boundary conditions of the drill during use. These conditions may change the transmission and dissipation of vibrations. While the effects of these human and environmental variables are documented in existing literature, they fall outside the scope of this study.

3.1.3.6 Resonant Characteristics of Components

Each structural element of the drill possesses a distinct natural frequency due to its geometric shape, its fixture and material properties. When the applied impact frequency or its harmonics approach these natural frequencies, the system exhibits susceptibility to resonance [13]. While specific values

may vary, components such as the handle, due to their flexibility and distance from the impact source, are particularly vulnerable to localized resonance phenomena during operational conditions.

3.2 Motivation for Analytical Modelling

Although experimental testing provides valuable insight into the vibrational behavior of the jackleg drill, it falls short in offering clarity about the internal transmission of forces and the role of individual components in shaping the overall dynamic behavior. An analytical model, even in its most basic form, is an essential tool for visualizing the propagation of mechanical energy through the structure and assessing how the properties of individual components might influence the system's response.

In this study, a simplified lumped-mass model was developed to represent the drill body as a system of lumped masses connected by springs and dampers. Due to missing parameters, a numerical solution wasn't performed; however, the model supports a qualitative understanding of how structural layout, component stiffness, and spatial arrangement may impact vibration amplitudes at various points along the drill. While the model simplifies motion along the axial direction, it complements the experimental setup, which captures vibration responses in all three axes (X, Y, Z), helping contextualize direction-specific behaviors.

This modeling approach was particularly helpful in guiding sensor placement, ensuring that measurements were taken in areas likely to exhibit varied vibratory behavior. It also establishes a conceptual framework for interpreting variations in amplitude and directional responses, particularly within the context of resonant and non-resonant conditions.

While the current model is not intended to replace experimental observations, it offers a simplified structural perspective that may serve as a foundation for a high-fidelity model in the future, to simulate dynamic responses and validate component behavior to explore potential design modifications aimed at vibration reduction.

3.3 Four-Lumped Mass Model

3.3.1 Schematics with Masses, Springs and Dampers

A simplified lumped-mass model was developed to model the dynamic behavior of the jackleg drill during operation. It included four lumped masses interconnected by linear springs and dampers. Each mass symbolizes the main structural components of the drill: Fronthead, Main Cylinder, Backhead and Handle. These components are arranged sequentially, enabling them to respond collectively to the internal excitation generated by the piston. Although the real system exhibits multi-directional motion, the model was limited to axial analysis due to modeling constraints. However, the schematic aligns with experimental sensor placements that captured vibration in all three axes.

As illustrated in Figure 3.3-1, the main cylinder housing the piston is subjected to a periodic input force produced by compressed air. While this force acts in the axial direction, the is designed to accommodate motion along all three axes, aligning with the orientations in which vibration data have been captured.

The connections between each adjacent pair of masses are characterized by:

- Springs- which represent the stiffness of the mechanical interfaces (such as threaded connections and structural contacts).
- Dampers- which account for the energy dissipation capabilities of these connections (including factors such as material damping, friction, and compliance)

Although the airleg is not explicitly modeled as a separate mass, it is assumed to provide external support to the main cylinder, thereby influencing the boundary conditions of the system. Its presence contributes to constrained motion near the forward end of the drill.

It is important to note that this schematic is not intended to reflect the physical geometry or exact dimensions of the drill; instead, it serves as a conceptual framework for understanding the mechanisms by which energy generated by the piston may propagate through the drill structure. This model facilitates the understanding of potential amplification or attenuation of vibration at different points within the system.

3.3.2 Mass, Stiffness and Damping Matrices

The model of the jackleg drill consists of four discrete masses interconnected by spring-damper elements, as illustrated in the schematic diagram. Each mass corresponds to a significant component of the drill assembly: the Fronthead, main cylinder, backhead, and the handle. For this model, as shown in Figure 3.3-1, the system is intentionally simplified to the axial direction only, which approximates the dominant force path of impact. This excludes bending, torsion, or lateral modes, which may be observed in Y and Z directions during experimental analysis. The stiffness and damping matrices are also formulated only for the axial direction, i.e. X-axis. Future models may extend this to multi-axial analysis once sufficient modal parameters are available.

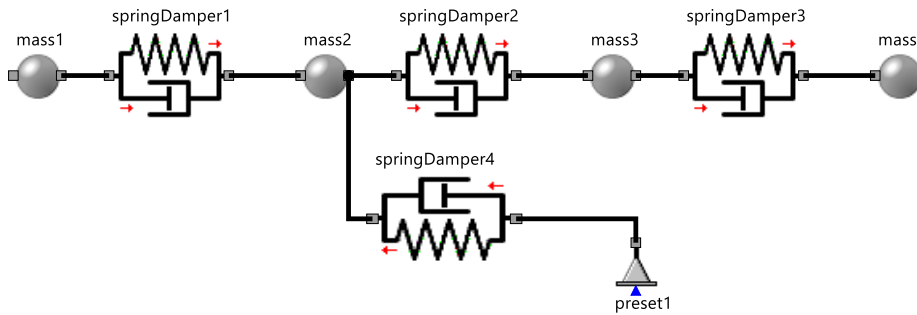


Figure 3.3-1 Low-fidelity 4-mass vibration model of the jackleg drill, showing mass–spring–damper representation with input excitation.

3.3.2.1 Equations of Motion

The simplified governing equations of motion for the horizontal vibration (i.e. X-direction), for each mass, were derived using Newton's second law, assuming linear spring-damper behavior between adjacent components and axial excitation from the piston.

1. Mass 1- Fronthead (m_1):

$$m_1 \ddot{x}_1 = -k_1(x_1 - x_2) - c_1(\dot{x}_1 - \dot{x}_2)$$

2. Mass 2- Main Cylinder (m_2 , with force input $F(t)$):

$$m_2 \ddot{x}_2 = k_1(x_1 - x_2) + c_1(\dot{x}_1 - \dot{x}_2) - k_2(x_2 - x_3) - c_2(\dot{x}_2 - \dot{x}_3) - k_4 x_2 - c_4 \dot{x}_2 + F(t)$$

3. Mass 3- Backhead (m_3):

$$m_3 \ddot{x}_3 = k_2(x_2 - x_3) + c_2(\dot{x}_2 - \dot{x}_3) - k_3(x_3 - x_4) - c_3(\dot{x}_3 - \dot{x}_4)$$

4. Mass 4- Handle (m_4):

$$m_4 \ddot{x}_4 = k_3(x_3 - x_4) + c_3(\dot{x}_3 - \dot{x}_4)$$

3.3.2.2 Mass Matrix $[M]$

The mass matrix is defined as a diagonal matrix, where each diagonal entry signifies the lumped mass of an individual component. Specifically, it can be expressed as follows:

$$[M] = \begin{bmatrix} m_1 & 0 & 0 & 0 \\ 0 & m_2 & 0 & 0 \\ 0 & 0 & m_3 & 0 \\ 0 & 0 & 0 & m_4 \end{bmatrix} = \begin{bmatrix} 5.88 & 0 & 0 & 0 \\ 0 & 12.58 & 0 & 0 \\ 0 & 0 & 5.34 & 0 \\ 0 & 0 & 0 & 3.16 \end{bmatrix} kg$$

Where,

- m_1 = mass of Fronthead
- m_2 = mass of Main Cylinder
- m_3 = mass of Backhead
- m_4 = mass of Handle

Mass estimates are derived from approximate physical dimensions and the known weights of each component. Notably, the airleg is not treated as a discrete mass; instead, it is conceptualized as a supportive constraint within the system. The diagonal structure reflects that the translational inertia of each subassembly is uncoupled in the simplified axial model.

3.3.2.3 Stiffness Matrix $[K]$

The stiffness matrix delineates the rigidity of the connections among the components, utilizing three spring elements. The system is regarded as linear and symmetric, which helps with analysis. An additional element that accounts for the airleg's support mechanism for the main cylinder is the spring-damper4.

$$[K] = \begin{bmatrix} k_1 & -k_1 & 0 & 0 \\ -k_1 & k_1 + k_2 + k_4 & -k_2 & 0 \\ 0 & -k_2 & k_2 + k_3 & -k_3 \\ 0 & 0 & -k_3 & k_3 \end{bmatrix}$$

Where,

- k_1 = stiffness between Fronthead and Main Cylinder $\approx 5.76 \times 10^9$ N/m
- k_2 = stiffness between Main Cylinder and Backhead $\approx 1.35 \times 10^9$ N/m
- k_3 = stiffness between Backhead and Handle $\approx 1.72 \times 10^9$ N/m
- k_4 = stiffness of airleg (between Main cylinder and Ground) $\approx 2.82 \times 10^3$ N/m

The stiffness values listed above were estimated using simple axial spring models based on material properties and joint geometry. Metallic connections between drill subassemblies were treated as steel bars or bolted joints, where stiffness was approximated by $k = EA/L$ with the effective cross-sectional area and engagement length taken from drawings. For bolted joints, the combined stiffness of the bolt stretch and compressed member was calculated, with multiple bolts modeled in parallel. The backhead - handle connection was simplified as a solid shank in axial compression. The airleg support was represented as a pneumatic spring using $k = \gamma P A^2 / V$, where pressure, bore diameter, and travel length were taken from manufacturer specifications. These simplifications yield approximate values in the correct order of magnitude, but uncertainties in geometry, load distribution, and material behavior mean that the results should be viewed as nominal. The detailed calculations and intermediate steps are provided in **Appendix C**.

3.3.2.4 Damping Matrix [C]

The damping matrix mirrors the structural format of the stiffness matrix, representing the energy dissipation occurring at the connections between the components. It can be expressed as:

$$[C] = \begin{bmatrix} c_1 & -c_1 & 0 & 0 \\ -c_1 & c_1 + c_2 + c_4 & -c_2 & 0 \\ 0 & -c_2 & c_2 + c_3 & -c_3 \\ 0 & 0 & -c_3 & c_3 \end{bmatrix}$$

Where,

- c_1 = Damping coefficient between Fronthead and Main Cylinder
- c_2 = Damping coefficient between Main Cylinder and Backhead
- c_3 = Damping coefficient between Backhead and Handle
- c_4 = Damping coefficient of airleg (between the Main cylinder and Ground)

The damping matrix mirrors the structural format of the stiffness matrix, representing the energy dissipation occurring at the connections between the components. Since direct damping coefficients were not obtainable from the available experimental data, the terms are retained in symbolic form. It

is assumed that metallic joints (fronthead - cylinder, cylinder - backhead) provide relatively low damping due to their rigid steel interfaces, whereas the handle region is expected to exhibit higher damping contributions owing to its flexibility and operator interaction.

3.3.3 Mathematical Formulation of Equations of Motion

The dynamic behavior of the simplified four-mass drill system can be expressed using the standard second-order matrix form of motion:

$$M\ddot{x}(t) + C\dot{x}(t) + Kx(t) = F(t)$$

Where:

- $x(t) = [x_1(t), x_2(t), x_3(t), x_4(t)]^T$ is the displacement vector representing the translational motion of the Fronthead, main cylinder, backhead, and handle, respectively.
- M , C , and K are the mass, damping, and stiffness matrices defined in section 3.3.2.
- $F(t)$ is the external force vector, consisting of periodic excitation applied only at the main cylinder due to the internal motion of the piston. The frequency of excitation corresponds to the operating impact rate of approximately 37.5 Hz (2250 BPM).

No external boundary constraints are assumed in this formulation. The handle is free to rotate about the z-axis due to the type of connection between the handle and backhead, and the system is treated as self-contained, with the airleg contribution already incorporated as a support stiffness and damping term acting on the main cylinder.

This formulation provides a structural foundation for understanding how vibrational energy introduced by the piston may propagate through the system and affect different components during periodic loading.

3.3.4 Generic Force Representations

The force input applied to the drill structure originates from the periodic motion of the piston, which impacts the main cylinder approximately 2250 times per minute. This corresponds to a fundamental frequency of around 37.5 Hz, although experimental observations have indicated slight deviations (peaks near 35 Hz), which remain within reasonable bounds of the assumed base frequency.

From a modeling perspective, this impact force can be considered a non-harmonic periodic input, as real piston forces resemble rectangular pulses or short-duration impulses rather than smooth sinusoidal waves. These discontinuous or impulse-like signals contain multiple harmonic components when decomposed using a Fourier series.

In this simplified model. The input force $F(t)$ is represented as a summation of all the harmonic components of its Fourier series:

$$F(t) = \sum_{n=1,2,3,\dots}^{\infty} F_n \sin(n\omega t)$$

$$\text{And } \omega = 2 \pi f$$

Where:

- F_n are the Fourier coefficients for each harmonic,
- n is the harmonic number,
- ω is the fundamental angular frequency
- f is the excitation frequency, approximately 37.5 Hz.

For this model, the input force is represented using the first four harmonics:

$$F(t) \approx F_1 \sin(1\omega t) + F_2 \sin(2\omega t) + F_3 \sin(3\omega t) + F_4 \sin(4\omega t)$$

This approach maintains analytical simplicity while explaining the complexity of the actual force function. The inclusion of harmonics will be justified by the observations of experimental data, where resonance was noted.

Although the exact shape and duration of the force pulses are not modeled, this representation allows the system to be analyzed under a more realistic excitation condition than a single-frequency sine wave. The harmonic content of the input force plays a key role in determining how different components respond, especially when their natural frequencies align with the included harmonic terms.

This approximation provides a foundation for qualitative understanding of multi-frequency excitation effects, while remaining consistent with the low-fidelity modeling framework used throughout this study.

3.3.5 Discussion of Non-Harmonic Periodic Excitation

In practical terms, the force exerted by the piston on the drill structure is not a smooth, continuous waveform; instead, it is a series of discrete, impulsive impacts. These impacts give rise to a periodic but non-harmonic force profile, characterized by a broad spectrum of frequency components that extend beyond the fundamental frequency.

In contrast to a pure sine wave, an impulsive or rectangular force signal introduces a complex array of higher-order harmonics, as elaborated in the previous section. The presence of these harmonics is an intrinsic consequence of the force shape and can interact with the structural dynamics of the drill in ways that a single-frequency input fails to account comprehensively.

The harmonic content within the applied force can lead the system to exhibit an enhanced vibratory response at frequencies beyond the fundamental. When any of the system's natural frequencies associated with individual components or their interactions align with these harmonic frequencies, localized resonance may ensue. This phenomenon is particularly significant for components that possess higher flexibility or are situated further from the excitation source, as they are more prone to amplifying the vibratory energy introduced by the higher harmonics.

One notable component in this context is the handle assembly, which is mechanically flexible and positioned at the farthest distance from the piston in the system. The inherent characteristics of the handle, coupled with the effects of harmonic excitation, may render it particularly susceptible to resonance. This aspect will be further investigated in the experimental analysis presented in Chapter 5.

3.4 Relations between Model and Drill Components

The low-fidelity model described in the previous sections was constructed to conceptually mirror the structure of the jackleg drill, with each lumped mass representing a distinct physical component. This mapping was developed to support a simplified understanding of how vibrational energy introduced by the piston might propagate through the system and concentrate in specific areas.

- Mass 1- Fronthead represented the interface through which the energy of the impact is transferred from the piston to the drill steel. As the initial point of force transmission to the external load (the rock), this component was expected to experience high input forces but limited vibration amplification.

- Mass 2- Main Cylinder modeled as the central housing that contains the piston and valve assembly. This is the point of force application in the model, consistent with the internal location where the piston delivers periodic impacts.
- Mass 3- Backhead served as the structural rear section of the drill and the interface for air and water input. Its primary contribution in the model was inertia and mass coupling between the main cylinder and the handle.
- Mass 4- Handle included in the model due to its structural flexibility and position furthest from the piston, i.e. the source of force. Its mechanical characteristics and location suggested a higher likelihood of amplification under certain frequencies, particularly if those frequencies matched its local modes. This motivated both its inclusion in the model and the placement of sensors during experimentation.

The mass-spring-damper representation, while simplified, reflects the relative arrangement and mechanical roles of these components. It provided a conceptual framework for anticipating vibrational behavior and informed the experimental strategy used to measure directional responses at different locations along the drill.

3.5 Limitations of the Model

While the four-mass low-fidelity model offers valuable insight into the possible vibration behavior of the jackleg drill, it is very important to acknowledge the limitations inherent in its formulation and intended use.

The model assumes one-dimensional translational motion, using linear springs and dampers to represent mechanical connections between components. As such, it does not capture more complex dynamics such as rotational effects, bending modes, or multi-axis coupling, which are likely to influence the real system's behavior. These simplifications were intentionally made to maintain analytical clarity and to align the model with the available information.

Damping values were not directly measured or extracted from empirical data; instead, they were included symbolically to represent qualitative energy dissipation at the interfaces of the components. Likewise, the stiffness values were not determined through experimental methods; they were assigned conceptually based on the relative rigidity between the various masses involved.

The input force was idealized as a periodic harmonic function or a Fourier sum, rather than deriving from actual pressure waveforms or time-resolved measurements of impact forces. This abstraction was required due to the limited access to internal force measurements and the practical constraints faced during testing.

No formal validation of the model was performed using experimental data, as the assumptions and resolution of the model were not sufficient to support a quantitative comparison. The model was therefore used strictly as a qualitative tool: to conceptualize how input forces may propagate, how structural layout affects response, and to support interpretation of non-resonant and potential resonant behaviors observed in physical testing.

Internal dynamics such as piston motion, valve switching and air flow control, though crucial to force generation, were intentionally excluded from the current model. Incorporating these elements would require a more detailed multi-physics approach that exceeds the scope of this study.

Despite these inherent limitations, the low-fidelity model effectively fulfilled its intended purpose by guiding the placement of sensors, framing observed vibrational responses, and providing structural insights. Future work may aim to develop a higher fidelity model that addresses these limitations, potentially allowing for predictive simulations, parameter-tuning, or component-level analysis.

Chapter 4:

Experimental Methodology

4.1 Purpose of Experimental Work

The primary objective of the experimental study was to investigate the sources of vibration and its propagation within the jackleg hammer drill, specifically to ascertain if the observed dynamic behavior is due to the impact forces or is influenced by the resonance phenomenon. This research aims to identify the dominant frequencies while quantifying their amplitudes across various parts of the drill. The focus is also on understanding the factors contributing to increased vibration levels at the handle. While considerable research has been done on examining the handle vibration levels and their implications for the operator's health, few studies- if any- have systematically measured and analyzed the vibration behavior across the multiple parts of the jackleg drill itself. This study aims to bridge that gap by providing a comprehensive assessment of vibration transmission throughout the drill body, thereby offering new insights into its dynamic behavior and potential avenues for design enhancements.

Contrary to previous studies that concentrated on the handle-hand interface, this study adopts a holistic perspective, treating the entire drill as an analytical subject. This broader approach is motivated by the need to reduce vibrations experienced by operators while circumventing the limitations of earlier mitigation approaches, which often faltered due to ergonomic and practical constraints.

Experimental tests were conducted on-site at the company's facilities, where the drill was operated by skilled technicians under both half and full throttle conditions to replicate typical operational scenarios. The data collected during these trials serves a dual purpose in the future: to understand the mechanical behavior of the drill and to provide critical input for the development and validation of a simulation model reflecting the drill's dynamic response in the future. The segmentation of the drill into four principal components for sensor placement was informed by preliminary simulations, which indicated these regions as zones with the highest amplitudes of vibration, thereby encouraging a detailed examination of vibration response throughout the drill. Moreover, the objectives of this experimental work are to inform vibration-safe drill redesigns that could help reduce operator exposure levels to below recommended limits, such as those outlined in ISO 5349-1. This

underscores the relevance of the study to regulatory standards such as ISO 5349-1, which sets out exposure limits and safety requirements for operators of vibrating machines.

4.2 Experimental Locations and Environment

Experimental testing for this study was conducted at the open ground at CANUN International’s Val Caron facility in Sudbury, Ontario. The tests were conducted outdoors on an open ground area, where a large Canadian Shield rock specimen, which is generally within the 6-7 range on the Mohs hardness scale [21]. It was positioned to function as the drilling surface. The jackleg drill was operated by qualified technicians from CANUN International for safety. Although conducting tests within an underground mine was impractical, the field setup effectively replicated critical operational factors, including but not limited to compressed air source, water supply system, and support for the airleg. All testing parameters- specifically air pressure, water flow, operator consistency, and environmental conditions- were maintained as much as possible. A schematic of the setup can be seen in Figure 4.2-1.

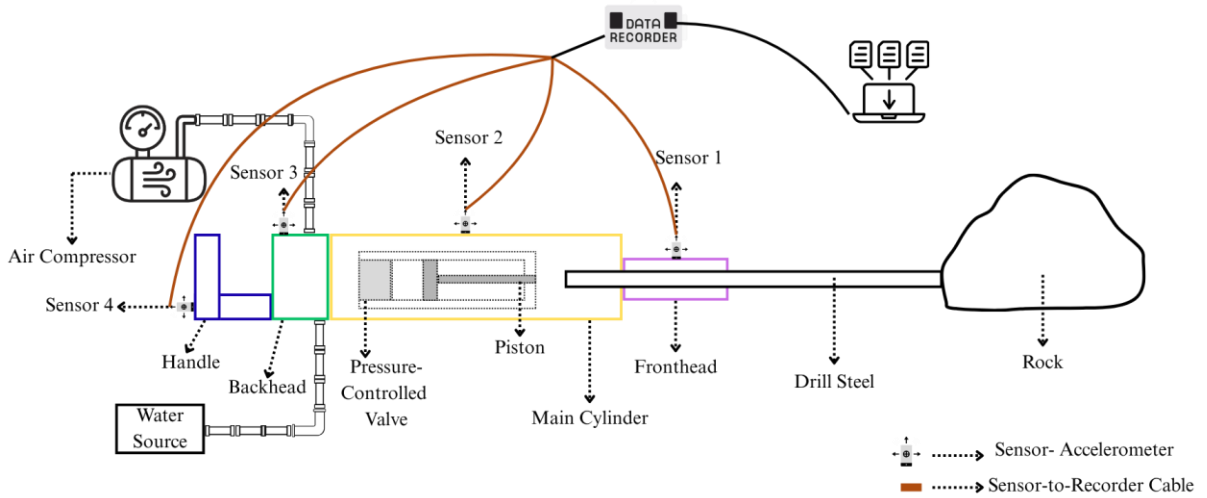


Figure 4.2-1 Schematic of sensor placement and data acquisition setup used during jackleg drill testing.

The environmental conditions prevailing during the testing sessions included temperatures ranging approximately from 21°C to 25 °C. While the outdoor setting introduced variables such as dust and minor moisture exposure, industrial-grade sensors with protective housing were used to ensure the reliability of the data.

All personnel present at the testing site followed strict safety protocols, including the use of hearing protection, protective goggles, and other necessary personal protective equipment, considering the high noise levels and dust associated with jackleg drill operation. To the best of the author's knowledge, no significant environmental factors compromised the integrity of the vibration measurements acquired during these experimental procedures.

4.3 Equipment and Instrumentation

4.3.1 Jackleg Hammer Drill

In this study, the jackleg hammer drill studied was the CANUN Model 260B, produced by CANUN International, located in Val Caron, Ontario, Canada. This specific model, as shown in Figure 4.3-1, is characterized by its cylinder diameter measuring 79.4mm and a piston stroke of 73.25mm, with an effective working piston stroke limited to 66.7mm. The average depth of the hole created during the 60-80 second intervals was about 76cm. The drill operates at a frequency of 2250 blows per minute, ensuring efficient penetration into various substrates. The overall length of the drill (handle to the fronthead) measures 686.0mm, and it weighs approximately 33.0kg, which is significant for portability and maneuverability.

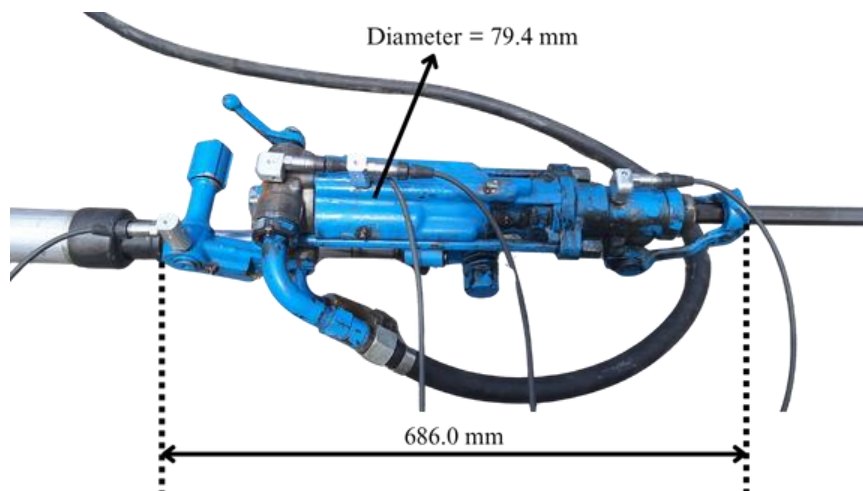


Figure 4.3-1 Basic Dimensions of Drill

The attached standard airleg used during the tests weighs 15.0kg and features a travel length of 1270.0mm, providing necessary support and stability during operation. Moreover, the drill works at an air consumption rate of approximately 4.9 cubic meters per minute when functioning under a

specified supply pressure of 90 psi, which was consistently maintained throughout the experimental procedures to ensure reliable performance.

For the drilling operations, standard drill steel dimensions were used with each piece measuring 22mm in diameter and 108mm in length. It is important to note that all experimental evaluations were carried out using the standard configuration of the drill, without any optional accessories attached to the drill.

4.3.2 Test Rig and Mounting Arrangements

During the testing, the jackleg drill was manually operated in a near-horizontal orientation, with the drill bit positioned against a large rock placed firmly on the ground as shown in Appendix A, Figure A.2. The airleg was connected to the drill and was supported by a wooden log positioned behind the airleg, thereby maintaining alignment of the drill and eliminating the need for manual force to drill into the rock. The rock specimen was of considerable size and mass, resting freely on the ground without additional constraints, as its weight was adequate to prevent significant movement during drilling operations.

The measurement setup consisted of four linear accelerometers; each connected via 10-foot cables to a data recorder and analyzer. To achieve tri-axial vibration measurements using linear sensors, custom-designed Aluminum sensor blocks were expertly machined to allow for sensor mounting along the X, Y and Z axes. These aluminum blocks were securely fastened to bolts welded at predetermined locations on the body of the drill, ensuring both a stable attachment and precise sensor orientation. This mechanical fixture method was suggested in the PCB Piezotronics manual [22], as the most accurate approach for capturing high-frequency vibration data accurately under the operational conditions associated with drilling.

No external vibration isolation measures were taken, as the primary aim of the study was to characterize the authentic vibration behavior of the drill in its unaltered state, establishing a baseline for potential mitigation strategies. Photographs and schematic diagrams of the experimental arrangement are presented in subsequent figures for detailed reference.

4.3.3 Sensors and Measuring Devices

Vibration measurements were conducted using four piezoelectric accelerometers (Model 603C01), manufactured by PCB Piezotronics, located in Depew, New York. These sensors are of the ICP®-

type uniaxial sensors designed with a ceramic shear sensing element, known for their stability and high-frequency response in industrial environments. These sensors were chosen specifically for their rugged build and their ability to withstand field conditions involving airborne dust and slight moisture, which were indeed present during testing.

Each sensor was pre-calibrated by the manufacturer and came with ISO/IEC 17025-accredited calibration certificates, ensuring confidence in the accuracy of the vibration measurements. The 603C01 sensors generate a low-impedance voltage signal powered by a constant-current source from the data acquisition unit. They were connected via 10-foot coaxial cables, providing direct transmission of the voltage signal without the need for any external signal conditioning apparatus.

For optimal measurement accuracy, the sensors were attached to custom-designed aluminum blocks that were precisely machined to allow for the orthogonal mounting of three sensors. This innovative arrangement enabled tri-axial measurements while using uniaxial sensors. The aluminum blocks were securely fastened to threaded bolts welded onto four strategically chosen locations on the drill: Fronthead, main cylinder, backhead, and handle. This stud-mounting technique ensures effective coupling and reliable transfer of high-frequency vibrations. A detailed summary of the specifications for these sensors is presented in Table 4.3-1.

Table 4.3-1 Specifications of the Uniaxial Accelerometer Used for Field Testing

Parameter	Value
Sensor Type	ICP® Uniaxial Accelerometer
Manufacturer	PCB Piezotronics
Model Number	603C01
Sensitivity	100 mV/g
Measurement Range	±50 g
Weight	18 grams
Frequency Range (±5%)	0.5 Hz – 10 kHz
Resonant Frequency	>30 kHz
Output Type	Voltage (IEPE – constant current)
Mounting Type	Stud Mount (10–32 UNF)
Operating Temperature	-54°C to +121°C
Connector Type	Coaxial top connector

4.3.4 Data Acquisition System

The vibration signals from the accelerometers were acquired using a Spider-20HE data acquisition system, specifications of which are listed in Table 4.3-2, developed by Crystal Instruments (Santa

Clara, CA, USA). The Spider-20HE is a compact, portable, high-resolution dynamic signal analyzer with four input channels, all of which were used simultaneously during each test to capture either multiple locations or multiple axes, depending on the configuration.

The system was set to sample at a constant rate of 2560 Hz across all experiments, which provided a frequency resolution of 0.625 Hz. The selected sampling rate of 2560 Hz provided a Nyquist frequency of 1280 Hz, well above the highest observed vibration components (<500 Hz). In addition, the Spider-20HE hardware incorporates built-in anti-aliasing filters on each input channel, ensuring that high-frequency noise above the Nyquist limit is attenuated and does not influence the FFT results. This setting was decided based on the expected dominant frequency range (up to ~500 Hz) and the need for accurate frequency-domain representation during the subsequent FFT-based analysis. The data was recorded and monitored using EDM (Engineering Data Management) software provided by Crystal Instruments, which integrates with the Spider-20HE hardware for real-time signal visualization, configuration, and export.

All recorded data was saved in spreadsheet-compatible formats such as .csv and Excel (.xlsx), ensuring accessibility for post-processing and MATLAB-based frequency analysis. Signal conditioning was handled internally within the Spider-20HE unit, as the ICP® accelerometers used provide a low-impedance voltage output and require only constant-current excitation, which the system supplies directly. No external filters, amplifiers, or conditioning units were required between the sensors and the DAQ system. All channels were synchronized internally by the device, ensuring accurate time-domain correlation across sensors.

Table 4.3-2 Data Acquisition System Specifications

Parameter	Value
Device	Spider-20HE
Manufacturer	Crystal Instruments
Input Channels	4 (used simultaneously)
Sampling rate	2560 Hz (configured)
Signal Conditioning	Internal (ICP® compatible)
Data Storage Format	.csv, Excel (.xlsx)
Software	EDM- Engineering Data Management

4.3.5 Data Acquisition Software

The data was recorded and analyzed using EDM- Dynamic Signal Analyzer software, developed by Crystal Instruments, which integrates directly with the Spider-20HE data acquisition unit. The

software provided real-time signal monitoring, configuration control, and automated FFT processing during the tests.

The sampling rate was set to 2560Hz for all experiments, with data blocks recorded every 1.6 seconds during acquisition. However, to retain raw time-domain data for post-processing analysis, the software configuration was modified to save unprocessed signals externally at 1-second intervals in .csv format. These files were later used for MATLAB-based analysis, while additional snapshots were reviewed in Excel for quick interpretation. The software was configured, as listed in Table 4.3-3, with a Hanning window, 4096-point FFT size and a 50% overlap ratio to enable frequency-domain analysis with a resolution of 0.625 Hz.

Table 4.3-3 DSA Software Settings used in Testing

Parameter	Value
Software	EDM- Dynamic Signal Analyzer
Sampling Frequency	2560 Hz
Block Duration	1.6 s (FFT), 1.0 s (raw data)
FFT Window	Hanning
FFT Size	4096 points
Overlap	50%
Frequency Resolution	0.625 Hz
Filters Applied	None (raw), thresholded during analysis

Although the raw data were not filtered during acquisition, an initial noise thresholding step was implemented during analysis, wherein acceleration values below 0.5 m/s² and frequencies below 5 Hz were considered insignificant and excluded to simplify the spectral interpretation. No additional digital filtering was applied; the FFT spectra were taken directly from the Spider-20HE output. This ensured that only physically meaningful vibration peaks were retained for further analysis while avoiding unnecessary post-processing.

4.3.6 Safety Equipment

All experimental testing was conducted with site-specific safety protocols developed by CANUN International, Val Caron. Personal protective equipment (PPE) was provided by the company and strictly enforced throughout the duration of testing. All personnel close to the drilling operation, including the technician operating the jackleg drill, wore ear protection, safety goggles, and closed-toe shoes. The technician was additionally equipped with gloves and a protective vest. Personnel positioned farther from the drill, including the author, adhered to standard PPE requirements and

maintained an observation distance of approximately 8 to 10 feet from the rock specimen, where the data acquisition system and laptop were placed on a mobile cart.

Due to the high noise levels generated by the drill and the potential for flying rock debris, strict non-interference protocols were enforced. The author was explicitly advised against approaching or handling the drill during its operation, given that such equipment requires certified operator training. The drilling was conducted by a qualified technician, who worked under the direct visual supervision of a designated site manager. In addition, the drilling system was equipped with a manually accessible air shutoff button to ensure immediate response in case of an emergency.

The outdoor testing environment required careful consideration of weather-related interruptions, particularly rain, which occasionally delayed drilling sessions. The testing site itself was level and generally devoid of hazards, with the rock specimen strategically positioned near the edge to ensure stability during repeated impact loading. These precautions collectively led to a safer and more efficient testing process, allowing for the integrity and reliability of the data collected.

4.4 Experimental Protocol and Procedures

4.4.1 Machine Segmentation and Sensor Placement Strategy

Building upon the drill segmentation introduced in Chapter 3, the practical application of sensor placement required the strategic positioning of accelerometers at four distinct locations along the drill body: the Fronthead, Main Cylinder, Backhead, and Handle. These segments were treated as non-overlapping zones, starting at the rock-facing end (Fronthead) and extending towards the operator (handle).

For the axis-specific tests, all four aluminum sensor blocks were installed simultaneously, with each block accommodating a single uniaxial accelerometer. In contrast, tri-axial measurements at individual sites utilized a single block configured to support three accelerometers arranged orthogonally. A standardized coordinate system, as shown in Figure 4.4-1, was adopted across all experimental conditions; the X-axis aligned with the drilling axis (along the drill steel), the Y-axis defined the vertical orientation (up-down), and the Z-axis indicated the lateral direction. (side-to-side). Consistency in sensor orientation was thoroughly maintained throughout all setups, ensuring replicability in alignment during each phase of testing.

During the experimentation, minor mounting challenges were encountered, notably at the front head where the sensor block exhibited a tendency to loosen under elevated vibration amplitudes. Requiring multiple torque adjustments. Consequently, the data obtained from the front head proved to be limited in comparison to that from the other sensor locations. In contrast, the main cylinder back head and handle yielded stable mounting solutions through the use of welded studs and secure fastening of the aluminum blocks, significantly enhancing the reliability of the data collected from these positions.



Figure 4.4-1 top view of the jackleg drill instrumented with accelerometers at multiple locations, and X, Y & Z axes defined.

4.4.2 Operational Test Configurations

The jackleg drill was tested under 2 distinct throttle settings: Full throttle and half throttle. These settings were determined by the physical position of the throttle lever operated by CANUN's technicians. While these positions were not quantitatively measured, they were consistently applied based on the technician's expertise and established internal operating standards.

Two main configuration sets of drill were tested- Full throttle and Half throttle. For each throttle setting, tests were structured in two parts: axis-specific measurements across the drill. (i.e., X, Y, and Z axes measured individually across all four components) and triaxial measurements performed at each component location (i.e., X, Y, Z at Handle, Backhead, Main Cylinder, and Fronthead).

Each configuration was repeated twice, yielding a total of 14 tests per throttle level, i.e. 28 valid test runs in total, and a detailed list of test runs can be seen in Table 4.4-1. Full throttle tests typically

lasted between 60 and 90 seconds. Whereas half-throttle runs were extended to approximately 2 minutes to accommodate the reduced frequency of impacts.

Although a greater number of runs were initially captured, the final analysis was limited to those tests with stable sensor contact and maintained signal integrity. Configurations identified with issues such as sensor detachment or electrical noise, particularly noted at the front head, were excluded from consideration. Test sequencing was planned to minimize environmental variation and maintain consistency in operator behavior and system conditions throughout the testing period.

Table 4.4-1 Summary of test runs conducted at full and half throttle settings, showing approximate duration, drill part tested, and axis orientation.

Throttle setting	Duration	Part Tested	Axis Tested
Full	48 s	All	X-X-X-X
Full	52 s	All	X-X-X-X
Full	53 s	All	Y-Y-Y-Y
Full	55 s	All	Y-Y-Y-Y
Full	54 s	All	Z-Z-Z-Z
Full	53 s	All	Z-Z-Z-Z
Full	22 s	Handle	X-Y-Z
Full	57 s	Handle	X-Y-Z
Full	58 s	Backhead	X-Y-Z
Full	58 s	Backhead	X-Y-Z
Full	54 s	Main Cylinder	X-Y-Z
Full	55 s	Main Cylinder	X-Y-Z
Half	120 s	All	X-X-X-X
Half	120 s	All	X-X-X-X
Half	120 s	All	Y-Y-Y-Y
Half	120 s	All	Y-Y-Y-Y
Half	120 s	All	Z-Z-Z-Z
Half	120 s	All	Z-Z-Z-Z
Half	120 s	Handle	X-Y-Z
Half	120 s	Handle	X-Y-Z
Half	120 s	Backhead	X-Y-Z
Half	120 s	Backhead	X-Y-Z
Half	120 s	Main Cylinder	X-Y-Z
Half	120 s	Main Cylinder	X-Y-Z

4.4.3 Measurement Procedures

Each test was initiated through a coordinated procedure to ensure alignment between the data acquisition system and the drill operation. Once all sensors were connected and the test configuration was finalized. The author manually initiated the recording on the Spider-20HE system, which was synchronized with the EDM software interface. A thumbs-up hand signal was then given to the drill technician, providing a buffer of approximately 3 to 5 seconds for the system to begin capturing baseline data before drilling. The technician operated the jackleg drill continuously while the author monitored signal quality in real-time. Upon completion of the desired duration, the author signaled the site manager, who instructed the technician to stop drilling, after which the recording was stopped immediately on the Spider-20HE device.

The timestamps were manually recorded in a field notebook by the author to enable cross-verification with signal traces in post-processing. These timestamps often aligned with notable changes in the RMS values during the tests, particularly when there were operational transitions or mechanical shifts. In addition to time records. Drilling depth was measured after each run using a standard tape measure placed along the drill steel. The depth values were relatively consistent across tests, typically averaging 70 ± 6 cm.

Observational notes were also maintained throughout testing to document issues such as sensor instability via strain or interruptions due to mounting problems. All tests were conducted by the same technician, who maintained a consistent crouched posture across runs, given the low height of the rock surface used for drilling.

4.5 Challenges and Limitations

During the testing phase, several practical challenges were encountered, particularly concerning the sensor mounting at the Fronthead of the drill. The high-frequency impacts and the limited flat mounting area hindered secure sensor placement, despite efforts such as repeated tightening and the use of custom aluminum blocks. In some cases, the mounting block loosened, while in others, the sensor detached completely during operation, resulting in approximately 6–8 instances where various configurations had to be discarded. Consequently, Fronthead data collection was minimized, with only essential runs conducted, and those with compromised sensor contact were excluded.

Although achieving perfect repeatability in test conditions was not feasible due to the outdoor operational setup, consistent testing protocols and repeated configurations were employed to maintain data reliability. While no formal validation dataset was available, internal comparisons and RMS trends reinforced the overall dependability of the data retained.

Chapter 5: Analysis, Results and Discussion

5.1 Data Preprocessing and Signal Conditioning

Proper signal conditioning and preprocessing were crucial in ensuring the quality and interpretability of the vibration data from the jackleg drill. The goal was to minimize the impact of noise and prepare the data for frequency domain analysis using Fast Fourier transform (FFT), while still accurately reflecting the operating conditions during data collection.

5.1.1 Noise Thresholding and Filtering

During data acquisition using the Spider system. No explicit filtering was applied. However, during post-processing, thresholds were established to identify and isolate significant vibration signals. Specifically, frequency components below 5 Hz were excluded during FFT analysis, an example of the same is shown in Figure 5.1-1, as they were considered unrelated to the drill's operational dynamics and likely reflected environmental influences or mechanical drift.

Additionally, acceleration signals with RMS values below 0.5 m/s^2 were considered to fall within the noise floor and were excluded from further spectral analysis. These noise thresholds were selected based on consistent patterns observed across multiple test runs, ensuring a thorough evaluation of the vibration data.

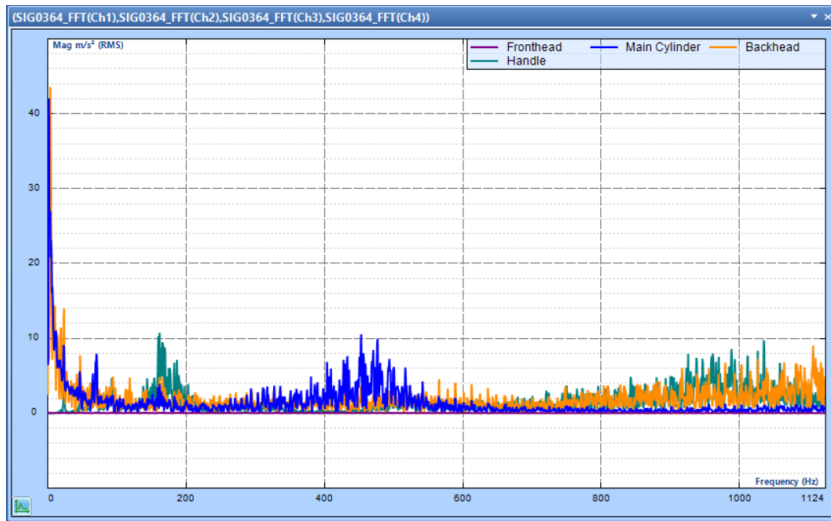


Figure 5.1-1 A Snapshot of the FFT of X-Axis across all Components

5.1.2 Run Selection and Consistency Verification

Each test configuration was conducted 2 times, acknowledging the inherent complexity of field conditions, which included factors such as power limitations, sensor detachment, or interruptions during drilling. As a result, achieving repeatability was not always guaranteed. Therefore, rather than averaging across trials, one representative run per configuration was selected based on a verification process involving the time domain RMS data, an example of which is shown in Figure 5.1-2.

The DSA software produced RMS vs time graphs for each run, effectively capturing the complete duration of the testing process. These graphs offered a clear visual representation of critical operational transitions. Such as collaring (the initial contact with the rock), sustained drilling, and retraction. Typically, these phases were marked by sharp changes in RMS values. The timestamps of these transitions were cross-checked against manually logged timestamps recorded during testing. If the observed RMS profile aligned with the expected operational sequence, the run was considered valid and used for further analysis.

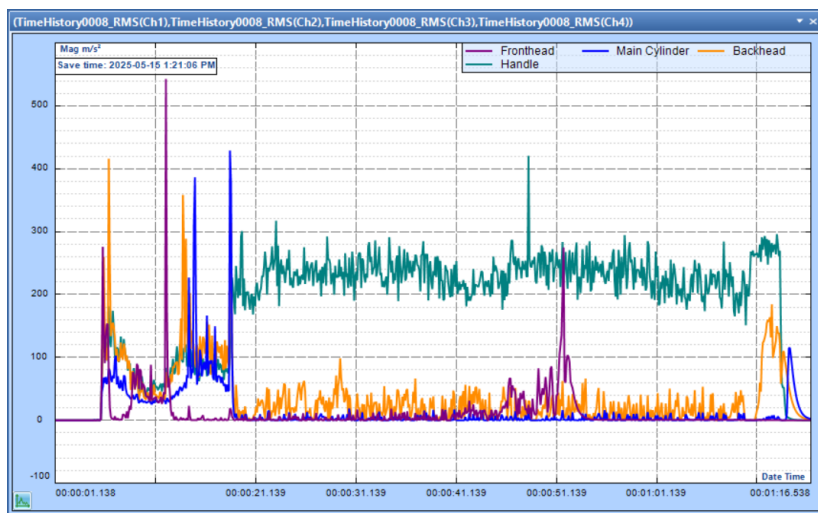


Figure 5.1-2 RMS Acceleration of X-Axis over the period of the test.

This approach allowed for qualitative validation of each data set, ensuring that the runs retained for analysis accurately reflected authentic and consistent drilling behavior. While statistical repeatability is limited, this method provides sufficient confidence in the representativeness of the selected data sets.

5.1.3 Configurations for Frequency Analysis

- *Configuration for data analysis*- For frequency-domain data analysis, the DSA software computed FFTs over time blocks/windows of 1.6 seconds. A 50% overlap was configured along with the application of the Hanning window function to each time block of data. These parameters, detailed in the acquisition settings outlined in Chapter 4, were carefully chosen to achieve an optimal balance between frequency resolution and temporal sensitivity. This approach results in the detection of both transient and sustained vibration features throughout the duration of the test.
- *Sampling Rate and Resolution*- The data was sampled at a rate of 2560 Hz, providing a frequency resolution of 0.625 Hz. The sampling rate was chosen to ensure sufficient capture of the fundamental impact frequency and its harmonics, which were expected to lie well above 20 Hz. The data was not down sampled at any point. During the analysis, thereby maintaining the integrity of the collected data and ensuring consistent resolution across all components and configurations.
- *Signal Quality Validation*- The internal consistency of the data was further verified by comparing axis-specific signals across different tests. For instance, the X-axis response recorded at the handle during axis-specific tests was cross-validated with corresponding axis data from the component-specific tests of the handle. The consistent pattern observation across these datasets confirms the reliability of the sensor's performance and ensures the validity of the measured signals. However, it is important to note that the vibration data collected from the Fronthead component frequently exhibited elevated noise levels and inconsistent profiles, especially due to repeated sensor detachment and mounting limitations. While some of the data from the Fronthead was retained for completeness, its accuracy was limited, and interpretations were made with caution.

5.2 Time-Domain Analysis

Time domain analysis provided an initial understanding of the drill's dynamic response during operation. Acceleration signals were plotted over the entire test duration for each sensor location and access, allowing direct observation of amplitude variations, transient events, and responsive characteristics across the drilling phases. These plots provided valuable insights into the magnitude and structure of vibrations prior to moving on to frequency-domain analysis.

5.2.1 Acceleration amplitudes and Component Response

The vibration amplitudes were demonstrated significantly across different components. The average root mean square acceleration levels along the X-axis were measured to range from approximately 11.8m/s^2 at the Fronthead to 184.3m/s^2 at the Handle. The Main Cylinder and Backhead exhibited intermediate levels with averages of 14.7m/s^2 and 35.9m/s^2 , respectively. In the Y & Z axes, the trends mirrored those of the X-axis, with the Handle consistently exhibiting the highest vibration response in all directional measurements. These measurements highlight the amplification of vibration as energy propagates through the structure from the impact zone towards the operator's grip point.

5.2.2 Observation of Drilling Phases

The time domain signals showed 3 distinct operational phases, namely, collaring, drilling, and retraction. These phases could be visually identified from the RMS vs time plots and raw acceleration data.

- Collaring- It is the process of making initial contact with the rock or making the initial hole. It generally lasts for 5 to 20 seconds and exhibits noticeably high and somewhat irregular RMS values. It is likely due to unstable contact dynamics at the onset of drilling.
- Drilling- This process mainly takes place for 50 to 60 seconds. Where the vibration signal becomes more stable and rhythmic, although with a lower overall RMS level than collaring and retraction.
- Retraction. It is the process of removing the drill steel from the rock. This process typically lasts for 5 to 10 seconds and shows another spike in RMS amplitude corresponding to the withdrawal of the drill steel from the hole.

This segmentation of processes not only validates the integrity of each data set as described in Section 5.1 but also shows the evolution of the drill's vibrational behavior with a change in operational conditions.

5.2.3 Transient Features and Signal Stability

Unexpected transients or anomalies were not observed within individual phases; however, transitions between operational states, for example, collaring to drilling or drilling to retraction, often resulted in

sudden amplitude shifts or changes in pulse regularity. These shifts were expected and reflect the real physical changes in contact dynamics and drill behavior in most of the selected runs; the absence of irregular spikes or drops confirms stable sensor operation and consistent signal acquisition.

5.2.4 Role of Time-Domain Analysis

Time domain plots serve as critical first steps in understanding the drill's vibrational behavior. They help in identifying major operational phases to validate the quality of recorded data and provide context for interpreting frequency domain results. In particular, the amplitude patterns and phase transitions evident in these plots guided the analysis of dominant frequencies and harmonics examined in Section 5.3.

5.3 Frequency-Domain Analysis

5.3.1 FFT and Spectral Behavior of Each Component

5.3.1.1 FFT method and Windowing

The frequency domain analysis was performed using Fast Fourier Transform (FFT) computed within the Dynamic Signal Analyzer (DSA) software during the data acquisition process. A fixed FFT window with a duration of 1.6 seconds, corresponding to 4096 data points at a sampling rate of 2560 Hz, was used alongside a Hanning window function. This approach ensured consistent spectral resolution and minimized spectral leakage, thereby enhancing the reliability of the frequency analysis. With a sampling rate of 2560 Hz, the Nyquist limit is 1280 Hz, well above the highest observed vibration frequencies (<500 Hz). No fold-over effects or unexpected peaks were observed, confirming that aliasing did not affect the FFT results.

5.3.1.2 Dominant Frequencies and Axis-Wise Behavior

FFT analysis for the Main Cylinder, Backhead, and Handle was conducted separately for each operational phase- Collaring, Drilling, and Retraction. All three axes of measurement- X, Y, and Z were analyzed.

- Collaring Phase- During the collaring phase, conducted at half throttle, the FFT analysis revealed a dominant frequency of approximately 23 Hz across all components. This frequency indicates a reduced impact rate compared to conditions at full throttle. Notably,

significant vibration magnitudes were detected in the X-axis, particularly in the Backhead and Handle, while the Main Cylinder exhibited comparatively lower amplitudes across all axes.

- Drilling phase- Under full-throttle drilling conditions, a clear fundamental frequency peak at 35.63 Hz was observed across all measured axes and components. The handle's X & Y axes in particular displayed strong vibration responses, indicating secondary harmonic peaks at approximately 71.5 Hz and 105 Hz. These harmonics suggest a complex response due to repetitive impacts during drilling operations. The Z-axis, in contrast, recorded lower amplitude vibrations across all components, highlighting its directional sensitivity to vibration transmission.

To support this observation, Table B.2 in Appendix B, presents the root mean square of magnitudes of the FFT signal peaks at dominant frequencies for the drilling phase. These values quantify the relative intensity of vibration at each component and axis, with prominent peaks seen at 35.63 Hz and its harmonics, especially for the Handle in the X-axis. A prominent peak in magnitude is also seen at 142 Hz, hinting at the possibility of resonance in the Handle assembly.

- Retraction phase- Analyzing the retraction phase revealed a significant increase in vibration amplitude at higher frequencies, especially in the handle. Dominant peaks in the handle's X-axis were observed within the range of 108-142 Hz, along with significant harmonic activity extending into higher frequency bands above 400 Hz. This shift indicates significant changes in dynamic conditions associated with the retraction process. The Main Cylinder and Backhead remained relatively lower in amplitude, indicating the localized amplification of vibrations at the handle.

5.3.1.3 Comparative Frequency Trends: Throttle and Operational Phase

Comparative analysis of the dominant frequencies shows that the operational conditions significantly influence vibration characteristics. The distinct shift from approximately 23 Hz during the collaring phase at half throttle to 35.63 Hz under full throttle drilling indicates a direct correlation between throttle levels and the frequency of piston impacts, reflected by the dominant FFT peaks observed.

5.3.1.4 Summary of Dominant Frequencies

Table B.1, Table B.2, and Table B.3 in Appendix B provide a concise summary of dominant frequencies and their corresponding magnitudes for each component during different operational phases.

This spectral analysis demonstrates the phase-dependent dynamic responses of the components, providing essential context for subsequent discussions concerning resonance, structural dynamics and vibration mitigation strategies.

5.3.2 Key Findings and Correlations

5.3.2.1 Peak Observations and System-Wide Trends

The FFT analysis revealed several consistent spectral characteristics across various components and operational phases of the system. In addition to the dominant impact frequencies at approximately 35.63 Hz at full-throttle and 23 Hz at half-throttle, prominent harmonics were observed around 70 Hz, 105 Hz, and 142 Hz, particularly in the handle's X-axis. These higher-order harmonics were less prominent in the Z-axis and exhibited moderate amplitude in the Y-axis, indicating a degree of directional selectivity in vibration response.

5.3.2.2 Comparisons across Throttle and Mounting Conditions

A clear difference in spectral content was observed between half-throttle and full-throttle operations. The full-throttle conditions produced stronger spectral amplitudes across most components and axes, with sharper and more defined peaks, particularly at the fundamental and the 1st and 2nd harmonics. In contrast, the spectral representation during half-throttle revealed lower overall magnitudes and a broader spectral distribution.

The mounting conditions remained consistent for all tested components except for Fronthead, which experienced sensor detachment during several runs. Consequently, its data was deemed unreliable and excluded from frequency-domain comparisons. The data sets for the Main Cylinder, Backhead and Handle were validated as reliable across all axes.

5.3.2.3 Physical Interpretation: Resonance and Vibration Response

Localized resonance behavior was particularly evident in the Handle component during retraction, as demonstrated by a pronounced peak around 142 Hz in the X-axis. This finding suggests structural

amplification or resonance at this frequency. Furthermore, there was a clear trend of increasing vibration magnitude observed from the Main Cylinder to the Backhead, ultimately ending at the Handle. Thereby confirming a progressive transmission of energy along the drill's structure towards the operator's grip point.

This energy propagation was especially prominent during drilling, where the root mean square (RMS) amplitude recorded for the Handle was nearly 11 times greater than that for the Backhead. This significant disparity was mirrored in the corresponding FFT peak amplitudes, reflecting an increase in vibration at the Handle.

5.3.2.4 Cross-check with Time-Domain Observations

The time-domain RMS data aligned with the findings from the frequency-domain analysis. For instance, during collaring, the RMS levels for the Handle and Backhead were relatively similar, aligning with the modest spectral peaks observed in the FFT analysis; however, during drilling, there was a pronounced increase in the RMS levels for the Handle, coinciding with the sharp spikes in frequency magnitude. This correlation further validates the interpretations regarding resonance phenomena and directional amplification.

This set of frequency-domain findings provides critical insights into vibration amplification, directional propagation, and the dynamics at the component level, establishing a strong basis for the interpretive discussions to follow in Chapter 6.

5.4 Vibration Response and Mapping

This section provides a qualitative overview of vibration response within the drill's structure derived from frequency-domain observations. It aims to summarize the evolution of vibration magnitudes among various components and to highlight the frequency at which specific behaviors are observed across different axes.

5.4.1 Directional Propagation Trends

During collaring, the highest vibration amplitudes were recorded in the Backhead, followed by the Handle and then the Main Cylinder. In contrast, during the drilling and retraction phases, the Handle consistently displayed the highest vibration levels, followed by the Backhead, while the Main

Cylinder exhibited the lowest amplitudes. This shift in vibration dynamics indicates the influence of contact conditions and operational phases on vibration transmission.

5.4.2 Resonant Frequency Zones

Throughout all experimental phases, a distinctly pronounced peak around 142 Hz was repeatedly detected along the X-axis of the Handle. This peak was not replicated in the measurements taken from the Backhead or the Main Cylinder and only exhibited a mild presence in other axes. The consistent occurrence and specificity of this peak indicate that the handle is likely experiencing resonance or localized amplification at this particular frequency.

5.4.3 Visualization and Mapping

To enhance the understanding of vibration dynamics, a vibration propagation map is developed to visually illustrate the intensity and relative transmission of vibrations between components across key frequency ranges. These maps, shown in Figure 5.4-1,2,3, are generated in MATLAB, and they serve as a valuable tool for visualizing how vibrational energy propagates through the drill's structure, thereby providing a clearer spatial representation of its behavior.

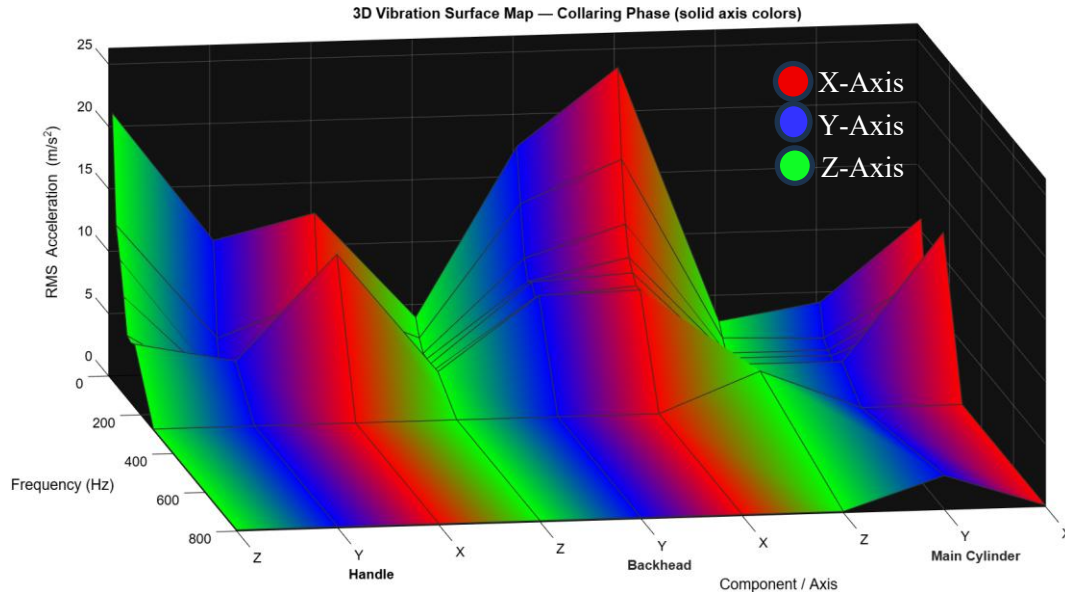


Figure 5.4-1 3D surface Heatmap for Vibration across Components and Axis during Collaring

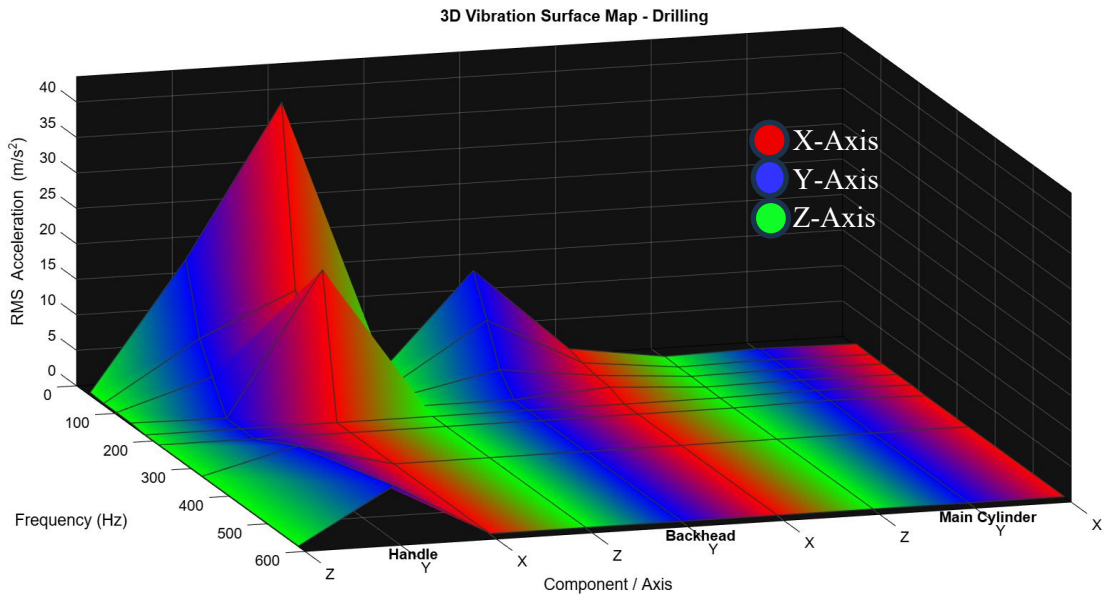


Figure 5.4-2 3D surface Heatmap for Vibration across Components and Axis during Drilling

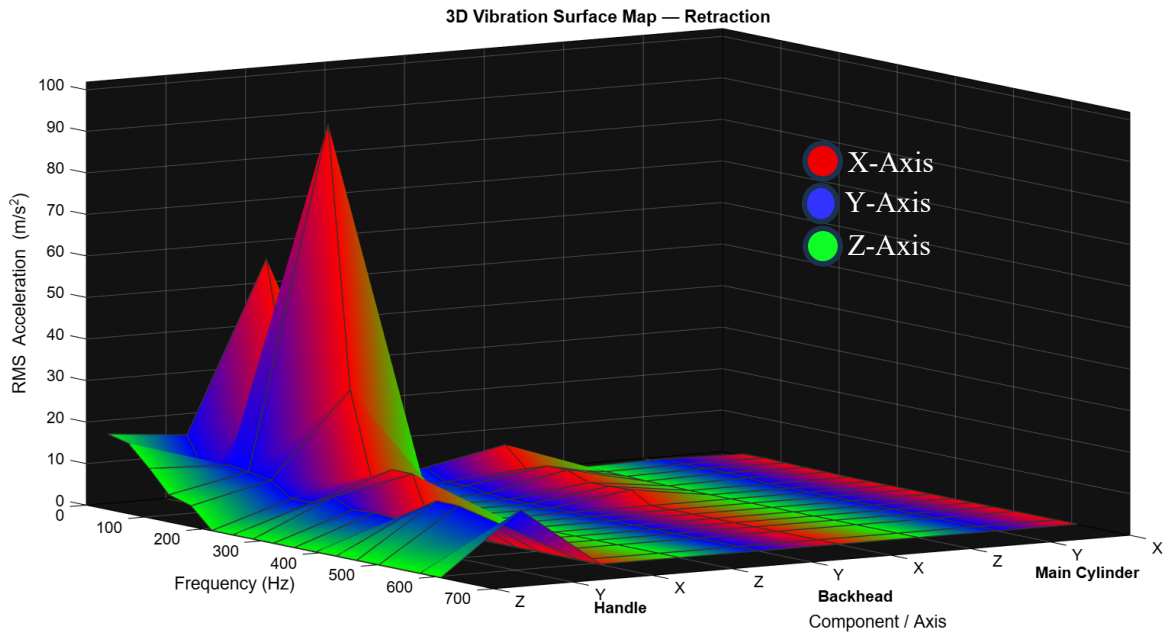


Figure 5.4-3 3D surface Heatmap for Vibration across Components and Axis during Retraction

5.5 Discussion of Results

5.5.1 Handle Vibration Characteristics

The handle, being the farthest point from the piston and the primary interface between the operator and the drill, exhibited the most intricate and amplified vibration patterns among all components. From a structural perspective, the drill can be approximated as a cantilever beam, with the drill bit and the airleg providing constrained support near the excitation source (the piston in the Main cylinder). This causes vibration amplitudes to increase toward the free end, where the handle is located, making it a focal point in the analysis of resonance and operator-experienced vibration. Data collected across the three operational phases- Collaring, Drilling, and Retraction- indicate that vibration levels at the Handle varied significantly by both axes and phase, suggesting the presence of resonance phenomena and directional amplification.



Figure 5.5-1 Mounted accelerometers on the Handle of the drill, showing orientation relative to the structural axis.

5.5.1.1 X-Axis

The X-axis, aligned with the drilling direction (penetrating the rock), with accelerometers mounted at the point nearest to the operator's holding position and far away to avoid interference, as shown in

Figure 5.5-1, consistently recorded the highest root mean square RMS acceleration values and exhibited dominant peaks at distinct frequencies throughout all three operational phases. During the drilling phase, the X-axis achieved a peak RMS value of 38.38m/s^2 at 35 Hz, with a notable peak of 16.5m/s^2 at 142 Hz observed, hinting at a potential resonance condition. Upon retraction, vibrations intensified further, peaking at 81.22m/s^2 at 143 Hz, significantly exceeding typical exposure limits and explaining a dynamic amplification effect.

The prominence of the X-axis response can be attributed to its alignment with the piston's impact direction, allowing for effective force transmission along the drill steel. Additionally, the Handle's geometry and its distal position from the main structural supports may have allowed it to act as a flexural mass. With less constraint, resulting in localized amplification at resonant frequencies, the consistently high amplitudes and harmonics observed in the X-axis reinforce the hypothesis that this axis is particularly susceptible to dynamic excitation and resonance buildup, especially during high-energy operating phases such as drilling and retraction.

5.5.1.2 Y-Axis

The Y-axis, defined as vertical (up-down movement), also exhibited notable vibration, particularly during the collaring phase, where unstable drill bit-rock contact likely led to unbalanced force transmission. The dominant frequency during this phase was 23 Hz, with the peak RMS of 9.6m/s^2 , indicative of early transient motion. In the drilling phase, this axis recorded moderate amplitudes such as 15.59m/s^2 at 35 Hz, while during retraction, values ranged between 5 and 13m/s^2 , suggesting partial transmission from structural or torsional components.

The moderate yet consistent response of the Y-axis is likely due to lateral rocking of the drill and slight shifts in the operator's grip posture, especially considering the technician was crouching throughout the operation, likely adding some variability in vertical stability.

5.5.1.3 Z-Axis

In contrast, the Z-axis, which represents side-to-side motion orthogonally to both the drilling and vertical directions, consistently exhibited the lowest vibration amplitudes among the three axes across the drilling and retraction phases. During drilling, the Z-axis RMS acceleration remained below 0.27m/s^2 across all dominant frequencies. However, during collaring, the Z-axis saw a maximum of

11.88m/s² at 23 Hz, being almost higher than values recorded for X & Y axes at comparable frequencies.

This anomaly in the collaring phase may be attributed to the lack of a stabilizing groove for the drill bit, which was created during the collaring phase. The creation of a groove restricted the lateral movement of the drill bit and consequently limited side-to-side vibration transmission during drilling and retraction phases. Furthermore, structural stiffness in this direction appears to offer enhanced damping characteristics.

5.5.1.4 Phase-wise Variation

A clear change in axis-wise vibration patterns, as shown in Figure 5.5-2, was observed as the drill progressed through different operational phases:

- Collaring- All three axes showed relatively comparable RMS values, suggesting that the initial lack of a defined groove in the rock surface caused the drill to wobble slightly in all directions. The drill bit had not yet seated fully, resulting in multidirectional transmission of transient impacts. This can be seen in Figure 5.5-2, and the relative data is in Table 5.5-1.
- Drilling- A strong directional preference became evident with the X-axis dominating. As the drill bit engaged firmly with the rock, the transmission became more unidirectional, aligning with the motion of the piston. This phase also showed indications of possible resonance, particularly at the frequency of 142 Hz. This can be seen in Figure 5.5-3, and the relative data is in Table 5.5-2.
- Retraction- X-axis values peaked sharply once again, potentially due to a temporary loss of contact between the drill bit and rock, resulting in pronounced recoil and instability. The Y & Z axes remained relatively stable, indicating that the dominant vibration during this phase remained axial in nature. This can be seen in Figure 5.5-4, and the relative data is in Table 5.5-3.

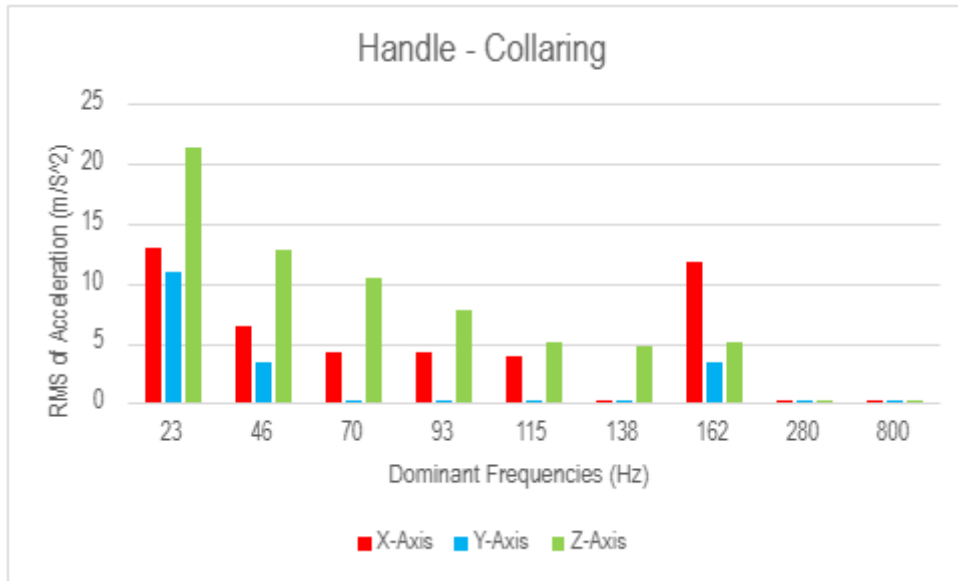


Figure 5.5-2 Dominant frequencies and average RMS acceleration in X, Y, Z axes at the handle during collaring phase.

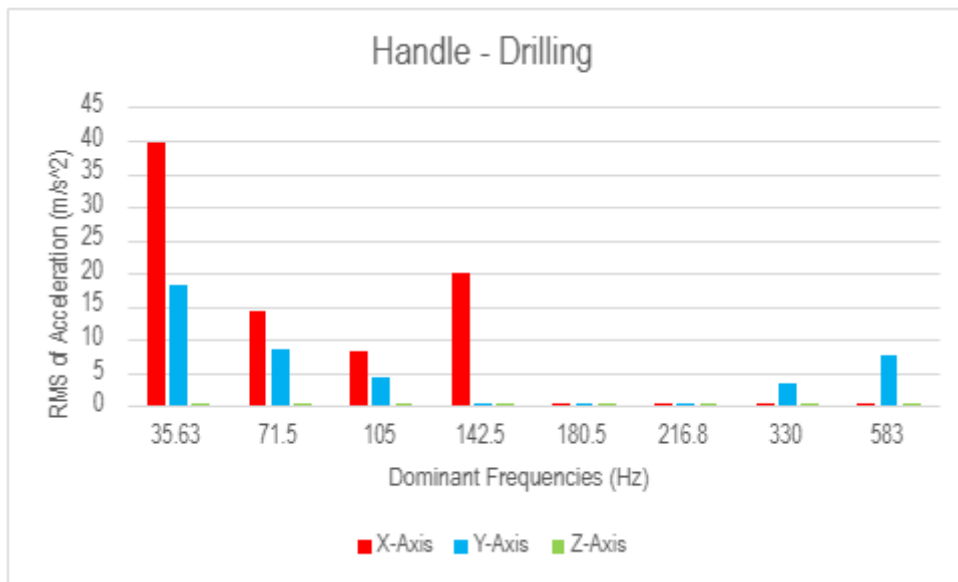


Figure 5.5-3 Dominant frequencies and average RMS acceleration in X, Y, Z axes at the handle during the drilling phase.

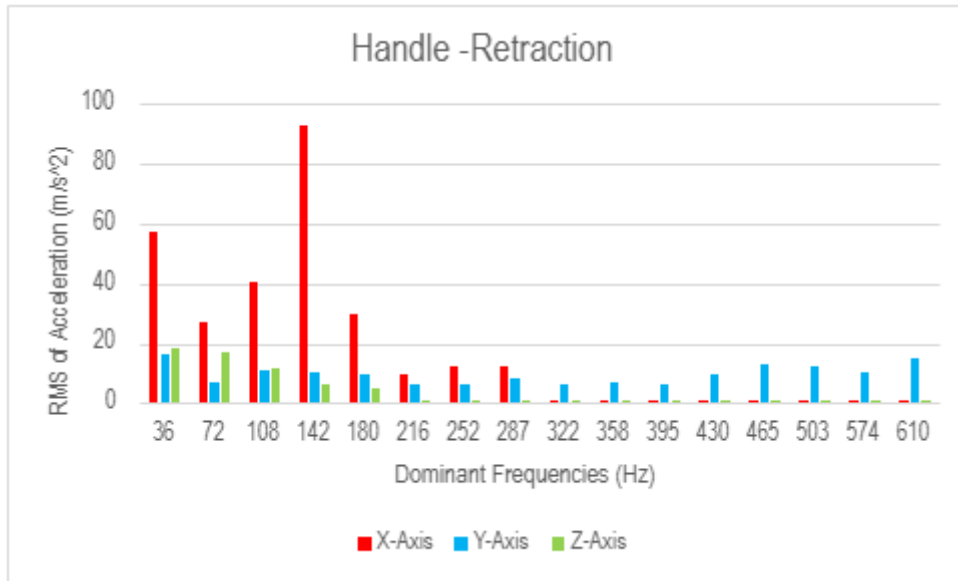


Figure 5.5-4 Dominant frequencies and average RMS acceleration in X, Y, Z axes at the handle during Retraction phase.

Table 5.5-1 Dominant frequencies and RMS acceleration values in X, Y, and Z axes at the handle during Collaring.

Collaring	X	Y	Z
23	12.941	10.978	21.438
46	6.406	3.505	12.821
70	4.277	0.100	10.416
93	4.188	0.100	7.794
115	4.010	0.100	5.036
138	0.100	0.100	4.830
162	11.795	3.472	5.072

Table 5.5-2 Dominant frequencies and RMS acceleration values in X, Y, and Z axes at the handle during Drilling.

Drilling	X-Axis	Y-Axis	Z-Axis
35.63	39.612	18.379	0.451
71.5	14.475	8.578	0.323
105	8.172	4.498	0.337
142.5	20.168	0.100	0.301
180.5	0.100	0.100	0.100
216.8	0.100	0.100	0.100
330	0.100	3.548	0.100

Table 5.5-3 Dominant frequencies and RMS acceleration values in X, Y, and Z axes at the handle during Retraction.

Retraction	X-Axis	Y-Axis	Z-Axis
36	57.164	16.336	18.191
72	27.380	7.307	16.944
108	40.642	11.144	11.924
142	92.593	10.525	6.573
180	29.681	9.494	5.003
216	9.759	6.159	0.100
252	12.566	6.229	0.100
287	12.552	8.594	0.100
322	0.100	6.507	0.100
358	0.100	6.861	0.100
395	0.100	6.489	0.100
430	0.100	9.633	0.100
465	0.100	12.789	0.100
503	0.100	12.685	0.100
574	0.100	10.341	0.100
610	0.100	14.745	0.100

5.5.2 Backhead Vibration Characteristics

The back head, located near the control interface of the jackleg drill, serves as a crucial transition zone for both air flow and operator input. While it does not directly absorb the impact of the piston, it effectively transmits structural and vibratory loads between the Main Cylinder and the Handle. This section analyzes the evolution of vibration in each axis throughout these operational phases and highlights notable directional trends.

5.5.2.1 X-Axis

Vibration along the X-axis, which aligns with the drilling direction, exhibited moderate amplitudes throughout all operational phases. During collaring, the vibration peaked at 15 m/s^2 at a frequency of 35.63 Hz. During the drilling phase, activity was observed at frequencies of 71.88 Hz and 105 Hz, with root mean square (RMS) values of 10.5 m/s^2 and 7.89 m/s^2 , respectively. These values are considerably lower than those recorded at the handle, indicating that while the Backhead does not serve as the primary site of amplification along the axis, it still plays a role in the transmission of directional forces.

The X-axis response can be attributed to the Backhead's proximity to the piston-valve system and its role as a load transition point between the Main Cylinder and Handle. Additionally, minor recoil during retraction may be transmitted through the Backhead before being amplified at the handle.

5.5.2.2 Y-Axis

The Y-axis, measured vertically, consistently exhibited higher RMS values compared to the X & Z axes across most operational phases. For instance, during the retraction phase, the Y-axis RMS peaked at 14.46 m/s^2 at a frequency of 105 Hz, indicating significant vertical oscillation. This could be due to dynamic rocking of the drill body during changes in feed force or operator-induced movement when the throttle valve mounted on the Backhead is adjusted.

In contrast to the Handle, which showed a dominant response along the X-axis, the Backhead appears to absorb and reflect vertical components, particularly during collaring and retraction when contact conditions with the rock are unstable or changing.

5.5.2.3 Z-Axis

Vibrations measured side-to-side along the Z-axis were generally of lower magnitude and exhibited less variability than those in the other two axes. During the drilling phase, RMS values ranged from

2.7 to 4.8m/s², further diminished during retraction. The relatively subdued response in the Z-axis can be attributed to the drill's enhanced lateral stability once a groove has been established in the rock face, which minimizes off-axis motion.

Additionally, the sensors' mounting location (away from the most flexible handle structure) contributed to the lower Z-axis response, as this direction is more effectively constrained near the drill body.

5.5.2.4 Phase-Wise Variation

- Collaring- During the collaring phase, vibrations across all three axes were somewhat elevated due to instability at the drill bit's contact point. The Y-axis exhibited a slight dominance, likely resulting from the vertical wobble as the drill bit began to sit. This can be seen in Figure 5.5-5, and the relative data is in Table 5.5-4.
- Drilling- Vibrations stabilize into consistent frequency bands in the drilling phase, with dominant peaks observed in the X & Y axes. The Z-axis maintained the lowest levels, confirming the overall lateral stability of the drill. This can be seen in Figure 5.5-6, and the relative data is in Table 5.5-5.
- Retraction- Both the X & Y axes recorded amplified values during retraction, particularly near frequencies of 105 to 143 Hz. This may indicate a transitional dynamic state as the drill disengages from the rock. While the Handle demonstrated peak resonance in the X-axis at this point, the Backhead also reflected this activity, but with moderate amplification. This can be seen in Figure 5.5-7, and the relative data is in Table 5.5-6.

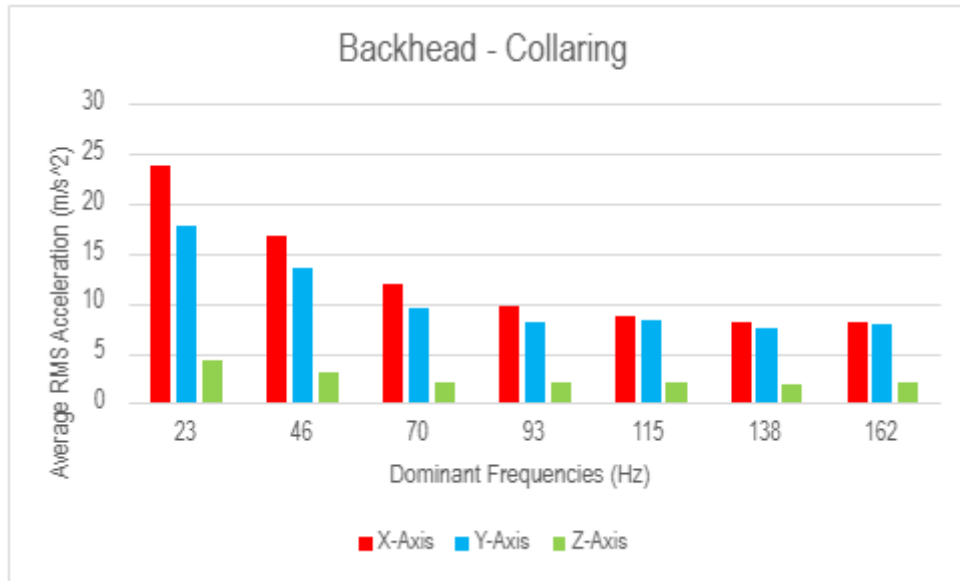


Figure 5.5-5 Dominant frequencies and average RMS acceleration in X, Y, and Z axes at the backhead during collaring phase.

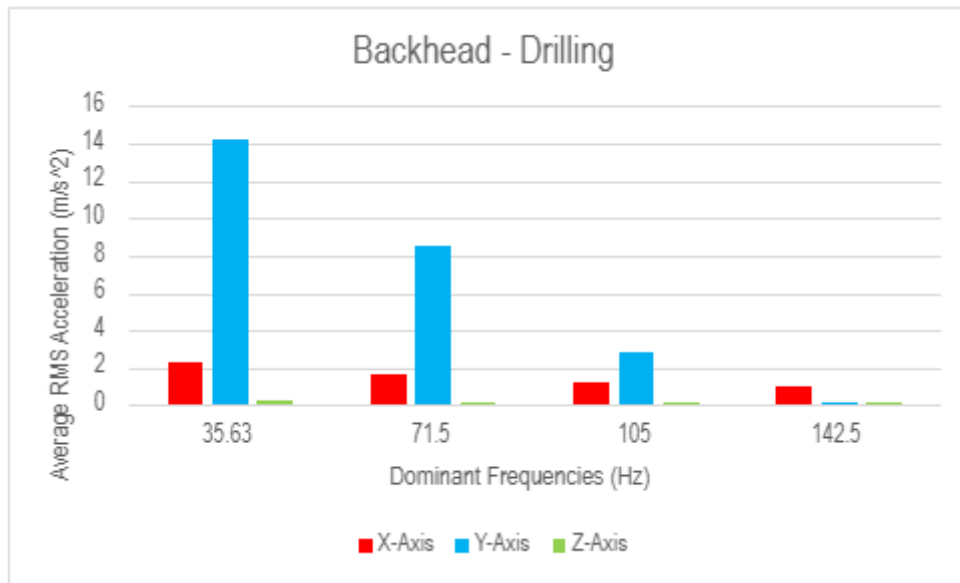


Figure 5.5-6 Dominant frequencies and average RMS acceleration in X, Y, and Z axes at the backhead during drilling phase.

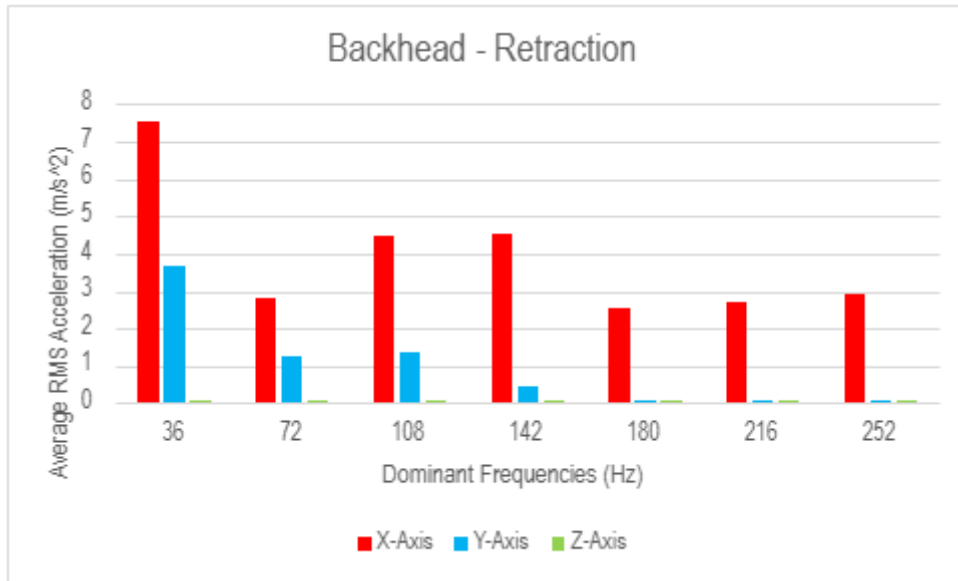


Figure 5.5-7 Dominant frequencies and average RMS acceleration in X, Y, and Z axes at the backhead during retraction phase.

Table 5.5-4 Dominant frequencies and RMS acceleration values in X, Y, and Z axes at the backhead during collaring phase.

Collaring	X-Axis	Y-Axis	Z-Axis
23	23.893	17.784	4.337
46	16.850	13.555	3.034
70	12.041	9.549	2.170
93	9.716	8.0455	2.095
115	8.827	8.342	2.028
138	8.146	7.447	1.888
162	8.181	7.995	2.131

Table 5.5-5 Dominant frequencies and RMS acceleration values in X, Y, and Z axes at the backhead during the drilling phase.

Drilling	X-Axis	Y-Axis	Z-Axis
35.63	2.270	14.170	0.220
71.5	1.680	8.550	0.180
105	1.210	2.870	0.100
142.5	1.010	0.100	0.100

Table 5.5-4 Dominant frequencies and RMS acceleration values in X, Y, and Z axes at the backhead during retraction phase.

Retraction	X-Axis	Y-Axis	Z-Axis
36	7.531	3.684	0.046
72	2.812	1.244	0.074
108	4.499	1.362	0.100
142	4.532	0.458	0.100
180	2.559	0.100	0.100
216	2.714	0.100	0.100
252	2.909	0.100	0.100

5.5.3 Main Cylinder Vibration Characteristics

The main cylinder forms the central body of the jackleg drill and houses some of the most critical components, such as the piston, valve assembly and internal air channels. Due to its inherent stiffness and mid-body placement, the Main Cylinder is instrumental in transmitting impact forces generated by the piston to both the Handle and the rock interface. Unlike the Handle and Backhead, the Main Cylinder was not physically touched or supported by the operator during testing, which makes it a useful reference for studying inherent structural transmission without ergonomic interference. The accelerometers were strategically mounted near the piston housing, specifically in the front-middle region of the cylinder

Overall, the Main Cylinder exhibited lower vibration amplitudes across all axes and operational phases. Supporting the hypothesis that it primarily acts as a transmission medium with relatively low amplification or resonance. However, distinct trends and directional behaviors were observed across the X, Y & Z axes.

5.5.3.1 X-Axis

In the X-axis, which is aligned with the drilling direction, the Main Cylinder exhibited relatively low root mean square (RMS) acceleration values throughout all operational phases. During drilling, the maximum recorded RMS acceleration was a mere 0.35 m/s^2 at a frequency of 35.6 Hz, a value significantly lower than those measured at the Handle or Backhead. This trend persisted during the retraction phase, where the peak RMS value reached 0.64 m/s^2 at 36 Hz. However, during collaring, a notable transient response was observed with a peak RMS of 11 m/s^2 at 23 Hz, likely attributed to transient impacts and initial instability of the drill bit.

These observations suggest that, although the Main Cylinder experiences substantial axial forces, it effectively dissipates energy, thus preventing amplification along the axial direction. This reinforces the idea that the resonance phenomena detected in the handle region does not originate within the Main Cylinder.

5.5.3.2 Y-Axis

The Y-axis, which is oriented vertically, showed the highest response among all axes at the Main Cylinder during most phases, particularly during collaring, where an RMS of 6.46 m/s^2 at 23 Hz was recorded. This may be attributed to the recoil force from initial contact with the rock surface and the slight upward tilting of the drill due to the buildup of the feed force.

During both drilling and retraction, the Y-axis values decreased to below 0.8 m/s^2 , indicating a stable structural alignment once the drill bit was securely seated. The vertical oscillations recorded during collaring suggested that these Y-axis vibrations are localized and transient rather than sustained or indicative of resonance.

5.5.3.3 Z-Axis

The Z-axis, representing side-to-side movement, exhibited a consistent and moderately active response throughout all operational phases. Interestingly, during collaring, the RMS value reached 4.3 m/s^2 at 23 Hz and again peaked at 3.7 m/s^2 at 800 Hz, hinting at some high-frequency excitation possibly related to the valve-piston interaction or natural material response.

In both the drilling and retraction phases, Z-axis values notably decreased, remaining below 0.5 m/s^2 , suggesting effective lateral damping. Considering the stabilizing groove of the drill bit and the

absence of external disturbances affecting the main cylinder, this Z-axis vibration likely reflects internal dynamic behaviors rather than amplification from external sources.

5.5.3.4 Phase-Wise Variation

Collaring- During this phase, all three axes exhibited elevated and variable amplitudes, particularly in the Y & Z axes. This behavior reflects transient instability and multidirectional impacts that occur upon initial engagement of the drill bit with the rock surface. This can be seen in Figure 5.5-8, and the relative data is in Table 5.5-7.

Drilling- During this phase, vibration levels stabilized, resulting in reduced amplitudes across all axes, with the main cylinder subsequently acting as a rigid intermediary devoid of observable resonance or amplification. This can be seen in Figure 5.5-9, and the relative data is in Table 5.5-8.

Retraction- During retraction, a slight increase in X & Z axes amplitudes was noted due to disengagement motion. However, all values remained below safety thresholds, maintaining an overall response that was low and well controlled. This can be seen in Figure 5.5-10, and the relative data is in Table 5.5-9.

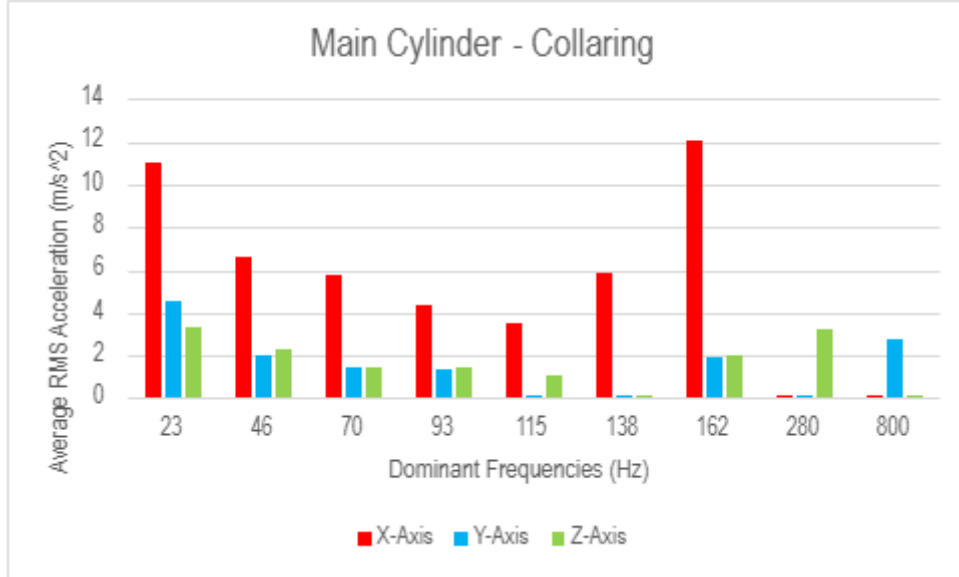


Figure 5.5-8 Dominant frequencies and average RMS acceleration in X, Y, and Z axes at the main cylinder during collaring phase.

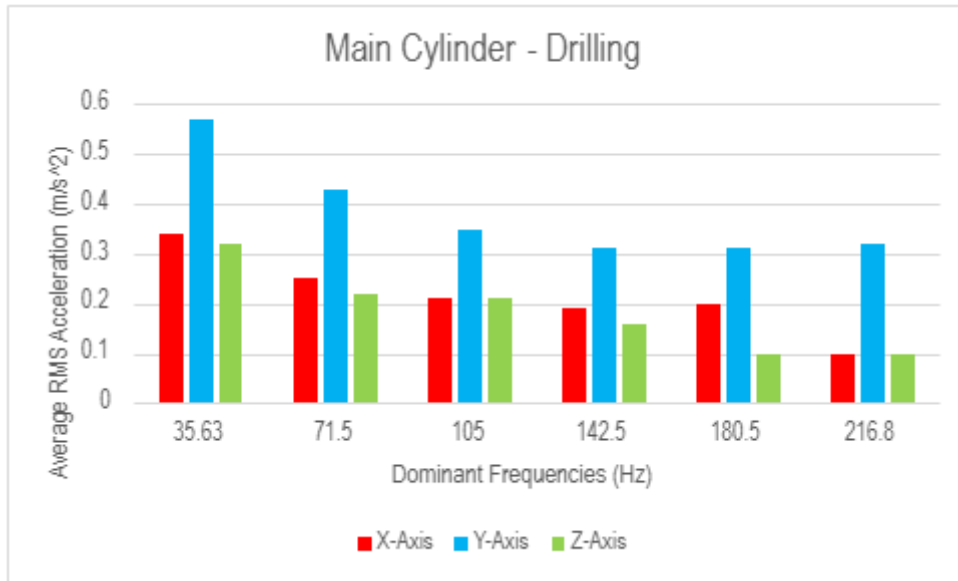


Figure 5.5-9 Dominant frequencies and average RMS acceleration in X, Y, and Z axes at the main cylinder during drilling phase.

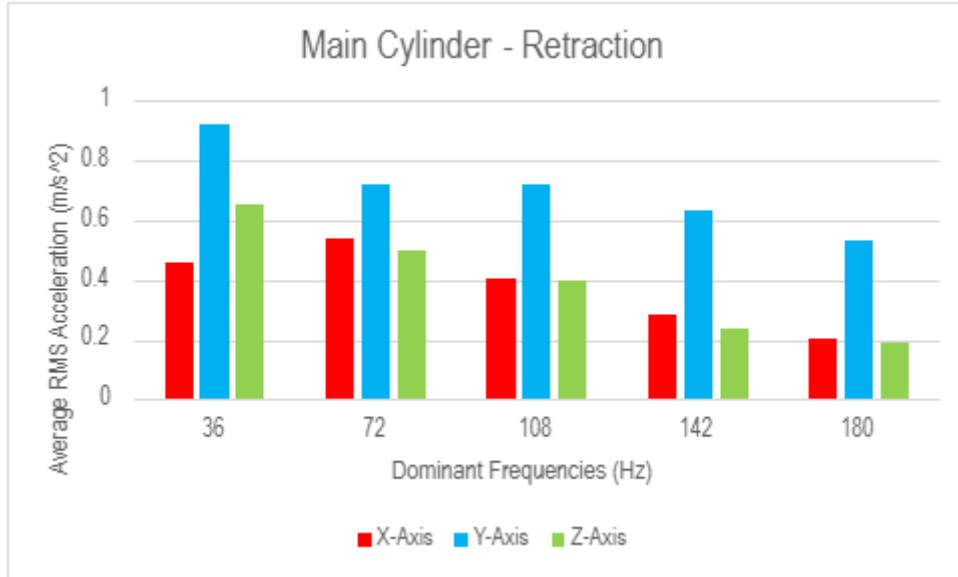


Figure 5.5-10 Dominant frequencies and average RMS acceleration in X, Y, and Z axes at the main cylinder during retraction phase.

Table 5.5-5 RMS acceleration values at dominant frequencies in X, Y, and Z axes at the main cylinder during collaring phase.

Collaring	X-Axis	Y-Axis	Z-Axis
23	11.029	4.561	3.286
46	6.640	2.042	2.291
70	5.784	1.432	1.453
93	4.402	1.366	1.414
115	3.482	0.100	1.031
138	5.877	0.100	0.100
162	12.101	1.932	1.999
280	0.100	0.100	3.270
800	0.100	2.732	0.100

Table 5.5-6 RMS acceleration values at dominant frequencies in X, Y, and Z axes at the main cylinder during the drilling phase.

Drilling	X-Axis	Y-Axis	Z-Axis
35.63	0.340	0.570	0.320
71.5	0.250	0.430	0.220
105	0.210	0.350	0.210
142.5	0.190	0.310	0.160
180.5	0.200	0.310	0.100
216.8	0.100	0.320	0.100

Table 5.5-7 RMS acceleration values at dominant frequencies in X, Y, and Z axes at the main cylinder during the retraction phase.

Retraction	X-Axis	Y-Axis	Z-Axis
36	0.462	0.922	0.652
72	0.542	0.719	0.500
108	0.403	0.718	0.401
142	0.288	0.635	0.235
180	0.206	0.533	0.190

5.5.4 Propagation In X-Axis

The analysis of the X-axis reveals a pronounced pattern of directional propagation. Vibrational intensities exhibit a progressive increase from the Main Cylinder to the Backhead and ending at the Handle. This trend effectively illustrates how axial forces generated by the piston travel along the drill body, experiencing partial damping in the main cylinder and amplification towards the operator's grip region.

Throughout all operational phases assessed, the handle consistently recorded the highest root mean square (RMS) values in the X-axis. Notably, peaks were observed at 36 Hz, 105 Hz, and with particular significance at 142.5 Hz. During the drilling phase, the handle registered 20.16m/s^2 at a frequency of 142.5 Hz, in stark contrast to the Backhead's 1.01m/s^2 and the Main Cylinder's 0.19m/s^2 . This dramatic increase in vibrational intensity supports the hypothesis that a localized resonance phenomenon occurs at the handle, presumably influenced by the structural boundary conditions or the configuration of the handle's mounting

Similar trends in directional amplification are evident during the collaring and retraction phases, even when the vibration levels of the Main Cylinder remained below 1m/s^2 , the Backhead exhibited vibrations in the range of 7 to 8m/s^2 , while the Handle frequently peaked above 25m/s^2 , which was particularly noted during retraction. These observations strongly indicate that the energy is not only transmitted but also undergoes structural amplification, likely due to compliance at joints, assembly interfaces, or the specific vibration modes induced by the geometry of the drill components.

5.5.5 Propagation In Y-Axis

In contrast to the dynamics observed along the X-axis, the propagation characteristics along the Y-axis displayed less consistency and provided weaker evidence of directional amplification. While some increase in amplitude was observed from the Main Cylinder to the Handle during collaring and retraction, this behavior did not persist clearly across phases or frequency bands.

For instance, during the collaring phase, the RMS acceleration in the Y-axis at 46 Hz increased from 2.4m/s^2 at the main cylinder to peak at 13.5m/s^2 at the Backhead and reduced to 3.5m/s^2 at the Handle. However, during drilling, the Handle recorded a peak at 18.4m/s^2 at 36 Hz frequency, while the Backhead and main cylinder were at 14.2m/s^2 and 0.6m/s^2 , respectively. This phase-specific variability indicates that vertical vibrations are potentially more influenced by factors such as the

operator's posture, feed force, or recoil dynamics rather than by straightforward structural transmission dynamics

Additionally, the Y-axis response appears less prone to resonance within the handle. Its values frequently remain below the defined limits when compared to the X axis. The absence of a consistent amplification pattern suggests that vibrations in the Y axis are predominantly transient, lacking significant structural amplification, except possibly during the collaring phase, when fluctuations and feed force may lead to uneven buildup.

5.5.6 Propagation In Z-Axis

The analysis of vibration propagation in the Z axis reveals the most damped vibration. Among the three evaluated axes. Throughout the various operational phases, the root mean square amplitudes consistently remained low across all components, rarely exceeding 1m per second square. During drilling, the Z-axis RMS recorded at 142 Hertz was measured at 0.1 m/s² at the handle, 0.1 m/s² at the backhead and 0.01 m/s² at the main cylinder.

Although a few high values were observed during collaring, for instance 12.43m/s² at the handle at 23 Hz, these were likely due to the early-stage instability before the drill bit settled into a groove in the rock. Once the drill bit engaged, the Z-axis response dropped significantly, confirming that lateral stability is achieved quickly and that the drill body resists side-to-side excitation effectively.

Importantly, no indications of resonance or amplification were detected in this directional assessment. This observation suggests that the structural rigidity and constraints present along the Z axis, combined with the symmetrical design of the drill body, play a Crucial role in limiting the lateral transmission of vibratory energy.

5.5.7 Suspected Resonance

Experimental investigations have identified a significant and consistent vibrational peak in the handle's X-axis response, particularly during the drilling and retraction phases, occurring within the frequency range of 142–143 Hz. Notably, this peak is either absent or minimal in the data gathered from the backhead and main cylinder, suggesting that the resonance phenomenon is localized within the handle rather than being a systemic issue.

The high root mean square (RMS) acceleration recorded at this frequency-20.16 m/s² during drilling and 29.69 m/s² during retraction, substantially exceeds the values measured in the

components at the front of the assembly. This observation is further corroborated by the absence of similar amplification in the Y or Z axes, or in the handle's response during the collaring phase. These findings indicate that the observed resonance behavior is not solely attributable to input frequencies but likely results from component-level resonance under specific operational conditions.

5.5.7.1 Contact- Based Resonance- A Hypothesis

Traditionally, resonance is associated with a component's intrinsic natural frequency. However, the evidence gathered here suggests that resonance may emerge from contact interactions between components rather than from the material properties or geometry of an isolated part. The interface between the backhead and the handle, which is secured by a nut-bolt connection, serves as a plausible candidate for this phenomenon.

Such interfaces can develop micro-gaps, variable stiffness, or compliance under load, leading to behavior that resembles a second-order spring-mass system, especially if the handle is effectively "floating" at certain frequencies due to insufficient constraint. This would explain why resonance is seen only during drilling and retraction, when dynamic forces are highest and contact conditions change, but not during collaring, when the system is more uniformly compressed.

The consistently dominant response in the X-axis also suggests that this resonance is directionally selective, driven by axial excitation and possibly amplified by the elongated geometry of the handle and its relative freedom compared to other masses.

Chapter 6:

Conclusion and Future Work

6.1 Summary of Major Findings

This thesis explored the vibration behavior of a jackleg rock drill using a combination of low-fidelity modeling and field experiments, with the objective of identifying component-level vibration patterns and potential sources of amplification or resonance.

6.1.1 Modeling Insights

- A simplified lumped mass-spring-damper model was constructed to conceptualize the segregation of the drill and vibrational characteristics of the system.
- This model highlighted the handle as a less constrained mass situated at the free end of the structure, thus indicating its vulnerability to resonance under specific loading conditions.
- Although precise resonance frequencies were not determined, qualitative assessments suggested the possibility of localized amplification occurring near the handle due to its positional dynamics and interaction with masses at the front of the assembly.

6.1.2 Experimental Findings

- Vibration data collected from critical components, including the main cylinder, backhead, and handle, revealed clear directional propagation, with the X-axis (aligned with the drilling direction) demonstrating predominant energy transfer.
- A distinctive resonance peak around 142 Hz was consistently observed in the handle's X-axis during both drilling and retraction phases; however, this peak was absent in components at the front of the assembly, suggesting a phenomenon of localized resonance.
- The Y-axis exhibited moderate and more transient vibrations, likely influenced by the operator's handling or feed force.
- In contrast, the Z-axis displayed low magnitude vibrations, reinforcing the notion of lateral stability and effective damping within that direction.

- The root mean square (RMS) values recorded at the handle frequently exceeded exposure thresholds specified in ISO 5349, particularly during drilling and retraction phases along the X-axis.
- The hypothesis of contact-based resonance, potentially resulting from the handle's bolted interface, was proposed and is supported by the frequency-specific, phase-dependent behavior observed.

6.2 Contributions of the Thesis

This thesis contributes significantly to the understanding of vibration response in jackleg hammer drills, moving beyond the traditional focus on handle-only measurements to a comprehensive, system-level analysis. Through a combination of experimental testing and conceptual modeling, the study mapped axis-wise and phase-wise vibration characteristics across multiple drill components, including the fronthead, main cylinder, backhead, and handle, under realistic operational scenarios.

A key contribution is the identification of a previously unreported resonance phenomenon localized at the handle assembly at approximately 142 Hz. Unlike fixed modal resonances, this amplification appears to result from dynamic interactions between structural components, particularly under full-throttle conditions. This insight presents new opportunities for targeted vibration mitigation strategies.

The study also demonstrated how a low-fidelity analytical model can support field experiments by guiding sensor placement in areas most likely to exhibit significant vibratory behavior. This integration of modeling and experimentation allowed for a more focused and interpretable data collection process.

Additionally, the research provides a valuable methodological framework for analyzing vibration response in similar pneumatic tools. The findings contribute to occupational health by supplying data that may be used to inform ergonomic redesigns and support compliance with standards such as ISO 5349-1. Importantly, this work offers a foundation for future engineering efforts aimed at reducing operator exposure through component-specific damping or redesign strategies, rather than relying solely on external vibration control accessories.

Collectively, these contributions position the study as a stepping stone toward both higher-fidelity modeling and practical vibration mitigation in underground drilling environments.

6.3 Limitations of the Current Study

The low-fidelity model did not include mode shape analysis or exact frequency prediction due to simplified assumptions and a lack of validated material data. Limitations in sensor mounting resulted in occasional detachment during tests, particularly at the Fronthead, thereby diminishing the available data at certain locations.

A consistent use of high-resolution tri-axial sensors across all components may have yielded deeper insights. Additionally, simulations were constrained by the absence of detailed CAD models and comprehensive material properties for the various drill components, which in turn limited the transition to high-fidelity analysis.

6.4 Recommendations

To build upon the findings and address the identified limitations, future research should focus on several key areas:

- **Improved Simulation Fidelity-** Development of detailed CAD-based models that incorporate realistic material and contact properties, alongside modal analysis and validation of predicted frequencies through experimental data.
- **Expanded Experimental Setup-** Installation of tri-axial sensors on additional components (such as the Fronthead, airleg, and drill steel) and execution of extended-duration tests across diverse operating conditions (including variations in throttle, grip force and rock types).
- **Mitigation and Design Improvements-** Investigation into the application of damping inserts or mechanical isolators between the handle and backhead to mitigate contact-based resonance. Exploration of modifications in handle geometry or decoupling strategies that could prevent rigid structural coupling in critical frequency ranges, as well as the design and testing of non-intrusive vibration isolation solutions that maintain drill performance while minimizing exposure to vibrations.
- **Ergonomic and Safety Evaluation-** Correlation of vibration exposure with miner grip, posture, and operating time utilizing risk models outlined in ISO 5349. Additionally, the evaluation of the potential for selective damping along the dominant axis (X-axis) should be considered without introducing excessive constraints on the overall system.

References

- [1] R. Oddo, T. Loyau, P. E. Boileau, and Y. Champoux, “Design of a suspended handle to attenuate rock drill hand-arm vibration: Model development and validation,” *J Sound Vib*, vol. 275, no. 3–5, pp. 623–640, Aug. 2004, doi: 10.1016/j.jsv.2003.06.006.
- [2] C. Kremer, D. Autenrieth, T. Stack, S. Rosenthal, and D. Gilkey, “Hand-Arm Vibration Controls for Jackleg Rock Drills: a Pilot Study Assessing Ergonomic Hazards,” *Min Metall Explor*, vol. 38, no. 5, pp. 1933–1941, Oct. 2021, doi: 10.1007/s42461-021-00451-6.
- [3] “MODULE NUMBER 10 OF INSTRUCTION GUIDE NUMBER 43 ON-THE-..OB TRAINING MODULES FOR SURFACE METAL AND NONMETAL MINES DRILL OPERATION.”
- [4] M. Bovenzi, “A longitudinal study of vibration white finger, cold response of digital arteries, and measures of daily vibration exposure,” *Int Arch Occup Environ Health*, vol. 83, no. 3, pp. 259–272, Mar. 2010, doi: 10.1007/s00420-009-0461-2.
- [5] “OSHA Technical Manual (OTM) - Section II: Chapter 3 | Occupational Safety and Health Administration.” Accessed: Jun. 29, 2025. [Online]. Available: <https://www.osha.gov/otm/section-2-health-hazards/chapter-3#HandArmVibration>
- [6] T. Clemm, K. C. Nordby, L. K. Lunde, B. Ulvestad, and M. Bråtveit, “Hand-Arm Vibration Exposure in Rock Drill Workers: A Comparison between Measurements with Hand-Attached and Tool-Attached Accelerometers,” *Ann Work Expo Health*, vol. 65, no. 9, pp. 1123–1132, Nov. 2021, doi: 10.1093/annweh/wxab051.
- [7] International Organization for Standardization, “Mechanical vibration- Measurement and evaluation of human exposure to hand-transmitted vibration- Part 2: Practical guidance for measurement at the workplace,” May 2001.
- [8] International Organization for Standardization, “Mechanical vibration- Measurement and evaluation of human exposure to hand-transmitted vibration- Part 1: General requirements,” 2015.
- [9] S. E. Keith and A. J. Brammer, “Rock Drill Handle Vibration: Measurement and Hazard Estimation,” *J Sound Vib*, vol. 174(4), pp. 475–491, 1994.

- [10] P. Marcotte, S. Ouellette, J. Boutin, P.-É. Boileau¹, G. Leblanc, and R. Oddo, “DESIGN OF A TEST BENCH TO EVALUATE THE VIBRATION EMISSION VALUES OF JACKLEG ROCK DRILLS.”
- [11] MIRARCO, “Experimental Test Report Jackleg Drill Handle Vibration Study,” Sudbury, Sep. 2015. [Online]. Available: www.mirarco.org
- [12] X. Fang, Y. Wang, Y. Zhang, and F. Li, “Experimental investigation on identification of lithologies and layered rock interface based on drilling vibration response,” *Geoenergy Science and Engineering*, vol. 233, Feb. 2024, doi: 10.1016/j.geoen.2023.212556.
- [13] S. S. . Rao, *Mechanical vibrations*. Prentice Hall, 2011.
- [14] M. R. Reksoprodjo and W. Nirbito, “Characteristics of Vibration Propagation on Passenger Car Monocoque Body Structure at Static Small Turbocharged Diesel Engine Speed Variation,” in *Journal of Physics: Conference Series*, Institute of Physics Publishing, Apr. 2020. doi: 10.1088/1742-6596/1519/1/012005.
- [15] D. J. . Inman, *Engineering vibration*. Prentice Hall, 2001.
- [16] H. Lindell, T. Clemm, and S. L. Grétarsson, “Vibration Reduction of Pneumatic Rock Drill for Rock Face Stabilisation Sector,” *Proceedings 2023, Vol. 86, Page 33*, vol. 86, no. 1, p. 33, Apr. 2023, doi: 10.3390/PROCEEDINGS2023086033.
- [17] S. Maeda, Y. Ye, and J. Tatsuno, “A STUDY ON PERFORMANE EVALUATION OF ANTI-VIBRATION GLOVES USING ON BODY HAND-TRANSMITTED VIBRATION MEASUREMENT”, Accessed: Aug. 05, 2025. [Online]. Available: <https://www.researchgate.net/publication/361637956>
- [18] G. ; Di *et al.*, “Comparison of Anti-Vibration Glove Performances in the Laboratory and in the Field: Similarities and Differences,” *Proceedings 2023, Vol. 86, Page 9*, vol. 86, no. 1, p. 9, Apr. 2023, doi: 10.3390/PROCEEDINGS2023086009.
- [19] P. Le, D. Xu, A. Vazhapilli Sureshbabu, and M. Zimmermann, “VIBRATION REDUCTION OF A HAMMER DRILL WITH A TOP-DOWN DESIGN METHOD,” in *Proceedings of the Design Society*, Cambridge University Press, 2023, pp. 3801–3810. doi: 10.1017/pds.2023.381.

- [20] A. V. Savilov, A. S. Pyatykh, and S. A. Timofeev, "Vibration suppression methods at high performance drilling," in *IOP Conference Series: Materials Science and Engineering*, Institute of Physics Publishing, Nov. 2019. doi: 10.1088/1757-899X/632/1/012108.
- [21] "Bill Cordua - Mohs' hardness testing of minerals and rocks." Accessed: Aug. 06, 2025. [Online]. Available: <https://www.mindat.org/article.php/1925/Mohs%27+hardness+testing+of+minerals+and+rocks>
- [22] PCB Piezotronics Inc., "Model 603C01 Platinum Stock Products; General purpose, industrial, ceramic shear ICP® accel, 100 mV/g, 0.5 to 10k Hz, top exit, 2-pin conn., single point ISO 17025 accredited calibration Installation and Operating Manual," 2023. Accessed: Jul. 09, 2025. [Online]. Available: www.pcb.com.

Appendix A

Test Site and Equipment Images



Appendix A 1 Uniaxial ICP® accelerometer (model 603C01) used for vibration data collection on the jackleg drill.



Appendix A 2 Technician operating the machine- depicting posture

Appendix B

FFT- Acceleration Magnitude- Frequency Tables

Collaring Dominant Frequencies (Hz)	Main Cylinder			Backhead			Handle		
	X	Y	Z	X	Y	Z	X	Y	Z
23	11.029	4.561	3.286	23.893	17.784	4.337	12.941	10.978	21.438
46	6.640	2.042	2.291	16.850	13.555	3.034	6.406	3.505	12.821
70	5.784	1.432	1.453	12.041	9.549	2.170	4.277	0.100	10.416
93	4.402	1.366	1.414	9.716	8.046	2.095	4.188	0.100	7.794
115	3.482	0.100	1.031	8.827	8.342	2.028	4.010	0.100	5.036
138	5.877	0.100	0.100	8.146	7.447	1.888	0.100	0.100	4.830
162	12.101	1.932	2.000	8.181	7.995	2.131	11.795	3.472	5.072
280	0.100	0.100	3.270	0.100	0.100	0.100	0.100	0.100	0.100
800	0.100	2.732	0.100	0.100	0.100	0.100	0.100	0.100	0.100

Appendix B- 1 RMS of Acceleration Magnitude (m/s²) at Dominant Frequencies during Collaring.

Drilling Dominant Frequencies (Hz)	Main Cylinder			Backhead			Handle		
	X	Y	Z	X	Y	Z	X	Y	Z
35.63	0.340	0.570	0.320	2.270	14.170	0.220	39.610	18.370	0.450
71.50	0.250	0.430	0.220	1.680	8.550	0.180	14.470	8.570	0.320
105	0.210	0.350	0.210	1.210	2.870	0.100	8.170	4.490	0.330
142.50	0.190	0.310	0.160	1.010	0.100	0.100	20.160	0.100	0.300
180.50	0.200	0.310	0.100	0.100	0.100	0.100	0.100	0.100	0.100
216.80	0.100	0.320	0.100	0.100	0.100	0.100	0.100	0.100	0.100
330	0.100	0.100	0.100	0.100	0.100	0.100	0.100	3.540	0.100
583	0.100	0.100	0.100	0.100	0.100	0.100	0.100	7.730	0.100

Appendix B- 2 RMS of Acceleration Magnitude (m/s²) at Dominant Frequencies during Drilling.

Retraction	Main Cylinder			Backhead			Handle		
Dominant Frequencies (Hz)	X	Y	Z	X	Y	Z	X	Y	Z
36	0.462	0.922	0.652	7.531	3.684	0.046	57.164	16.336	18.191
72	0.541	0.719	0.500	2.812	1.244	0.074	27.380	7.307	16.944
108	0.403	0.718	0.401	4.499	1.362	0.100	40.642	11.144	11.924
142	0.288	0.635	0.235	4.532	0.458	0.100	92.593	10.525	6.573
180	0.206	0.533	0.190	2.559	0.100	0.100	29.681	9.494	5.003
216	0.100	0.100	0.100	2.714	0.100	0.100	9.759	6.159	0.100
252	0.100	0.100	0.100	2.909	0.100	0.100	12.566	6.229	0.100
287	0.100	0.100	0.100	0.100	0.100	0.100	12.552	8.594	0.100
322	0.100	0.100	0.100	0.100	0.100	0.100	0.100	6.507	0.100
358	0.100	0.100	0.100	0.100	0.100	0.100	0.100	6.861	0.100
395	0.100	0.100	0.100	0.100	0.100	0.100	0.100	6.489	0.100
430	0.100	0.100	0.100	0.100	0.100	0.100	0.100	9.633	0.100
465	0.100	0.100	0.100	0.100	0.100	0.100	0.100	12.789	0.100
503	0.100	0.100	0.100	0.100	0.100	0.100	0.100	12.685	0.100
574	0.100	0.100	0.100	0.100	0.100	0.100	0.100	10.341	0.100
610	0.100	0.100	0.100	0.100	0.100	0.100	0.100	14.745	0.100

Appendix B- 3 RMS of Acceleration Magnitude (m/s²) at Dominant Frequencies during Retraction.

Appendix C

Stiffness Calculations

Material Constants (used throughout)

- Steel (SAE 8620) Young's Modulus: $E = 200 \text{ GPa} = 2.00 \times 10^{11} \text{ N/m}^2$
- Air specific heat ratio: $\gamma = 1.4$
- Absolute pressure for 90 PSI (information on pressure provided by CANUN) gauge:
 $P_{\text{abs}} \approx 90 \times 6894.76 + 101325 \approx 7.21 \times 10^5 \text{ Pa}$

C.1 Fronthead - Main Cylinder Stiffness k_1

Assumptions & Inputs (based on CAD and components information given by CANUN)

- Two bolts, radius $r_b = 0.98 \text{ cm} = 9.8 \text{ mm}$ (so $d_b = 19.6 \text{ mm}$)
- Bolt grip length $L_b = 1.43 \text{ cm} = 0.0143 \text{ m}$ (thickness of the clamped faces)
- Annular interface (compressed member) outer diameter $D_o = 6.508 \text{ cm} = 0.06508 \text{ m}$, inner diameter $D_i = 5.08 \text{ cm} = 0.0508 \text{ m}$
- Compressed member thickness $L_m = 0.0143 \text{ m}$ (same as bolt grip)

Step 1- Bolt stiffness (per bolt)

$$A_b = \pi r_b^2 = \pi (9.8 \times 10^{-3})^2 = 3.017 \times 10^{-4} \text{ m}^2$$

$$k_b = \frac{EA_b}{L_b} = \frac{(2.00 \times 10^{11})(3.017 \times 10^{-4})}{0.0143} = 4.22 \times 10^9 \text{ N/m}$$

Two bolts in parallel: $k_{\text{bolts}} = 2k_b = 8.44 \times 10^9 \text{ N/m}$

Step 2- Compressed member stiffness

$$A_m = \frac{\pi}{4} (D_o^2 - D_i^2) = \frac{\pi}{4} (0.06508^2 - 0.0508^2) = 1.300 \times 10^{-3} \text{ m}^2$$

$$k_{\text{member}} = \frac{EA_m}{L_m} = \frac{(2.00 \times 10^{11})(1.300 \times 10^{-3})}{0.0143} = 1.82 \times 10^{10} \text{ N/m}$$

Step 3- bolts and annulus are in series

$$\frac{1}{k_1} = \frac{1}{k_{bolts}} + \frac{1}{k_{member}} \Rightarrow k_1 = (8.44 \times 10^9) \parallel (1.82 \times 10^{10}) = 5.76 \times 10^9 \text{ N/m}$$

C.2 Main Cylinder - Backhead Stiffness k_2

Assumptions & Inputs (based on CAD and components information given by CANUN)

- Single through bolt, diameter $d_b = 2.54 \text{ cm} = 25.4 \text{ mm}$
- Grip length $L_b \approx 60 \text{ mm}$
- Compressed member approximated as a cylinder of effective diameter $D_g \approx 50.8 \text{ mm}$, length $L_m = L_b$

Step 1- Bolt stiffness

$$A_b = \frac{\pi d_b^2}{4} = \frac{\pi(0.0254)^2}{4} = 5.067 \times 10^{-4} \text{ m}^2$$

$$k_b = \frac{EA_b}{L_b} = \frac{(2.00 \times 10^{11})(5.067 \times 10^{-4})}{0.060} = 1.69 \times 10^9 \text{ N/m}$$

Step 2- Compressed member stiffness

$$A_m = \frac{\pi D_g^2}{4} = \frac{\pi(0.0508)^2}{4} = 2.027 \times 10^{-3} \text{ m}^2$$

$$k_{member} = \frac{EA_m}{L_m} = \frac{(2.00 \times 10^{11})(2.027 \times 10^{-3})}{0.060} = 6.76 \times 10^9 \text{ N/m}$$

Step 3- bolt and annulus are in series

$$\frac{1}{k_2} = \frac{1}{k_b} + \frac{1}{k_{member}} \Rightarrow k_2 = (1.69 \times 10^9) \parallel (6.76 \times 10^9) = 1.35 \times 10^9 \text{ N/m}$$

C.3 Backhead – Handle stiffness k_3

Assumptions & inputs (based on CAD and components information given by CANUN)

- Handle shank diameter $d = 1.00 \text{ in} = 25.4 \text{ mm}$
- Engagement depth $L = 2.312 \text{ in} = 58.77 \text{ mm} = 0.05877 \text{ m}$
- No soft bushing; tight fit (axial load path through steel)

Calculation:

$$A = \frac{\pi d^2}{4} = \frac{\pi}{4} (0.0254^2) = 5.067 \times 10^{-4} \text{ m}^2$$

$$k_3 = \frac{EA}{L} = \frac{(2.00 \times 10^{11})(5.067 \times 10^{-4})}{0.05877} = 1.72 \times 10^9 \text{ N/m}$$

C.4 Main Cylinder - Ground (Airleg) stiffness k_4

Assumptions & inputs (based on CAD and components information given by CANUN)

- Bore $D = 67 \text{ mm} = 0.067 \text{ m} \rightarrow$ piston area $A = (\pi D^2) / 4$
- Travel $L = 1270 \text{ mm} = 1.27 \text{ m}$ (gas length used for volume)
- Operating pressure $P_{\text{abs}} \approx 7.21 \times 10^5 \text{ Pa}$
- Single gas chamber, adiabatic $\gamma = 1.4$

Formula:

$$A = \frac{\pi D^2}{4} = \frac{\pi}{4} (0.067^2) = 3.52 \times 10^{-3} \text{ m}^2$$

$$V = AL = (3.52 \times 10^{-3})(1.27) = 4.47 \times 10^{-3} \text{ m}^3$$

$$k_4 = \gamma \frac{P_{\text{abs}} A^2}{V} = \frac{(1.4)(7.21 \times 10^5)(3.52 \times 10^{-3})^2}{4.47 \times 10^{-3}} = 2.82 \times 10^3 \text{ N/m}$$

Substituting the above k_i into

$$[K] = \begin{bmatrix} k_1 & -k_1 & 0 & 0 \\ -k_1 & k_1 + k_2 + k_4 & -k_2 & 0 \\ 0 & -k_2 & k_2 + k_3 & -k_3 \\ 0 & 0 & -k_3 & k_3 \end{bmatrix}, \text{ yields}$$

$$[K] \approx \begin{bmatrix} 5.76 \times 10^9 & -5.76 \times 10^9 & 0 & 0 \\ -5.76 \times 10^9 & 7.11 \times 10^9 & -1.35 \times 10^9 & 0 \\ 0 & -1.35 \times 10^9 & 3.07 \times 10^9 & -1.72 \times 10^9 \\ 0 & 0 & -1.72 \times 10^9 & 1.72 \times 10^9 \end{bmatrix} \text{ N/m}$$

(The $+k_4 = 2.82 \times 10^3$ term is negligible at this scale.)